

Geochemical Characterization and Temporal Changes in Parietal Gas Emissions at Mt. Etna (Italy) During the Period July 2000 - July 2003

Giovanella Pecoraino^{1,*} and Salvatore Giammanco¹

(Manuscript received 4 October 2004, in final form 20 July 2005)

ABSTRACT

Several types of natural gas emissions (soil gas, low temperature fumaroles, gas bubbling in mud pools) were collected monthly on Mt. Etna volcano between July 2000 and July 2003 both from its summit and its flanks. Samples were analysed for the determination of the concentrations of CO₂, CH₄, He, H₂, CO as well as the isotopic ratios of ¹³C/¹⁴C of CO₂ ($\delta^{13}\text{C}$) and He (R/Ra). The analysed gases were chemically divided into two groups: air-contaminated (from sites closer to the summit vents of Mt. Etna) and CO₂ - rich. Among the latter, samples from the lower SW flank of the volcano showed high contents of biogenic thermogenic and/or microbial CH₄. Isotopic shift in the $\delta^{13}\text{C}$ values is caused by input of organic CO₂ and/or by interaction between magmatic CO₂ and shallow ground water as a function of water temperature and CO₂ flux from depth. Based on a graphic method applied to $\delta^{13}\text{C}_{\text{TDC}}$ of some ground water, the inferred isotopic composition of the pristine magmatic gas at Mt. Etna is characterised by $\delta^{13}\text{C}$ values ranging from -2 to -1‰.

During the period July 2000 - July 2003 significant variations were observed in many of the investigated parameters almost at all monitored sites. Seasonal influences were generally found to be negligible, with only a limited effect of air temperature changes on soil CO₂ and ground temperature in only two of the air-contaminated sites. The largest chemical anomalies were observed in the air-contaminated sites, probably because of the strong buffering power of local ground water on gases released through the most peripheral areas where the CO₂-rich sites are located. The anomalous changes observed during the study period can be explained in terms of

¹ Istituto Nazionale di Geofisica e Vulcanologia - Sezione di Palermo, Palermo, Italy

* *Corresponding author address:* Dr. Giovannella Pecoraino, Istituto Nazionale di Geofisica e Vulcanologia - Sezione di Palermo, Via Ugo La Malfa 153, Palermo, Italy;
E-mail: g.pecoraino@pa.ingv.it

progressive gas release from separate batches of magma that ascend towards the surface in a step-wise manner. Data relevant to the period following the 2002-03 eruption suggest that magma kept accumulating beneath the volcano, thus increasing the probability of a new large eruption at Mt. Etna.

(Key words: Mt. Etna, Geochemistry, Gases, Eruptive activity)

1. INTRODUCTION

Mount Etna is the largest volcano in Europe (~1200 km² of total surface with a maximum height of ~ 3300 m above sea level) and is one of the most active in the world. A prominent feature of Etna's activity is the persistent emission of a huge volcanic plume arising from its four summit craters ("Voragine", "Bocca Nuova", South-east and North-east, see Fig. 1) both during quiescent and eruptive magma degassing. Other types of gas manifestations (mofettes, "mud volcanoes", diffuse soil degassing, bubbling gases in surface and ground water) also occur in peripheral sectors of the volcano. Many studies in the last years have focused particularly on soil degassing (Aubert and Baubron 1988; Allard et al. 1991; D'Alessandro et al. 1992, 1997a; Anzà et al. 1993; Giammanco et al. 1995, 1997, 1998a, b, 1999; Parello et al. 1995; Baubron 1996; Bruno et al. 2001; Caracausi et al. 2003a, b). Anomalous soil gas emissions in the Etna area occur mostly, if not exclusively, along active tectonic structures. Carbon dioxide (CO₂) is generally the most abundant species emitted, but several other gases (methane, helium, hydrogen, carbon monoxide, radon) can be found as well, with concentrations well above those in the air. The origin of CO₂ is magmatic, with a very small contribution from biogenic and/or organic sources. The temporal variations in the concentrations of some of these soil gases, and in particular in the efflux of CO₂, have shown significant correlations with variations in volcanic activity.

In this paper we present original data on the temporal evolution of the chemical and isotopic characteristics of gases collected simultaneously from low-temperature (T < 100°C) fumaroles, soil emissions, mofettes and mud volcanoes in and around the Mt. Etna area. Data were collected during the period July 2000 - June 2003. The results were compared to the temporal evolution of Etna's volcanic activity in a period of particularly strong eruptive events.

2. FIELD OBSERVATIONS, SAMPLING AND ANALYTICAL METHODS

Gas samples were collected from July 2000 to June 2003 in six sites in the Mt. Etna area (Fig. 1). The sampling frequency varied from once a month to twice a week, depending on the state of volcanic activity. RNE, TDF and BLV are fumarole emissions located close to the summit of the volcano (altitude > 2000 m a.s.l.) (Fig. 1); they are characterised by emissions of water vapour with outlet temperature generally lower than 100°C (RNE and BLV) or by diffuse soil gas anomalies accompanied by a weak thermal anomaly in the ground (TDF). In

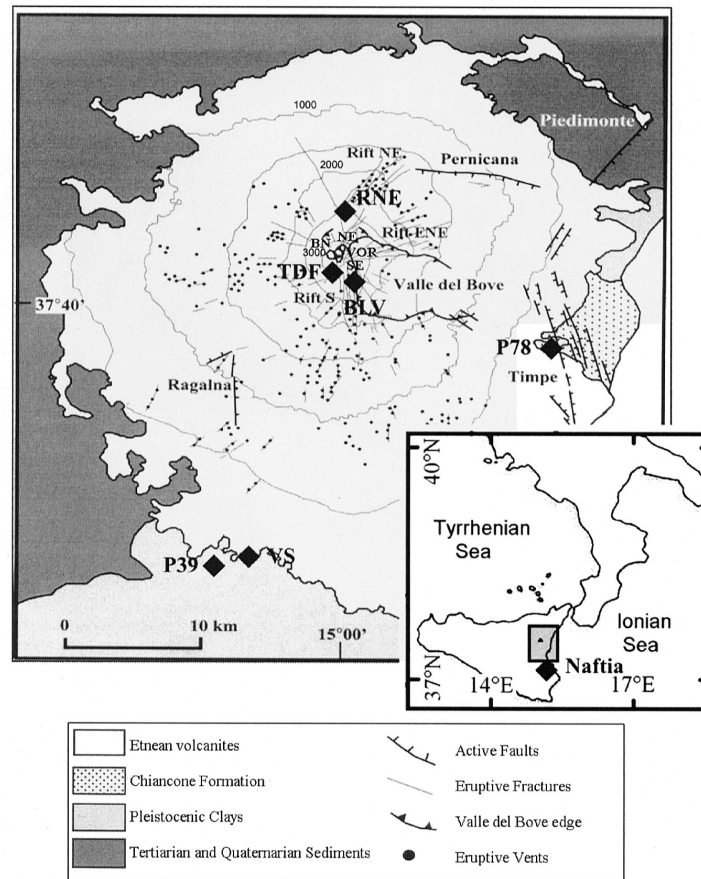


Fig. 1. Location of sampled gas emissions in the Etna area (solid diamonds). Altitudes in metres.

particular, RNE is located along the so-called NE rift. This volcano-tectonic feature consists of a group of eruptive fissures, radial in respect to Etna's summit, located on the upper north-eastern slope of the volcano, between 2500 and 1300 m of altitude. According to Giammanco et al. (1999), fumaroles in this area release magmatic gas through fractures connected with the main feeding conduit of the volcano. TDF is located near the summit craters (altitude of 2750 m a.s.l.), some metres south of the Torre del Filosofo hut (now buried by the tephra emitted during the 2002 eruption). It is connected to an active N-S-trending volcano-tectonic structure that belongs to the so-called SE Rift, and is probably related to the main feeding conduits of the volcano (Giammanco et al. 1998a). The site of BLV is also located along the SE Rift, at altitude of 2720 m a.s.l., but along a different fracture than that feeding TDF gas emissions. The BLV fumarolic field formed during the 1991-93 eruption where the 1991-93 eruptive fissure crossed the edge of the Valle del Bove morphological depression (Fig. 1). Site P78 is

located on the lower eastern flank of the volcanic edifice about 3 km east of the village of Zafferana Etnea, at an altitude of about 320 m a.s.l. It is characterised by anomalous emissions of soil gases along an inferred fault directed about WNW-ESE. Furthermore, in this site both CO₂ efflux and CO₂ concentration showed a high variability in relation with volcanic activity (Giammanco et al. 1998a). Based on the temporal variation of combined soil CO₂ degassing and crater plume SO₂ flux (Bruno et al. 2001), anomalous soil degassing at site P78 originates from magma stored in a relatively shallow level (5 - 10 km deep) of the magma column inside the main feeding conduits of Etna. Site P39 is located on the lower southwestern flank about 2 km southwest of the town of Paternò (altitude of about 115 m a.s.l) and approximately 20 km SSW of Etna's summit craters. It is a mofette characterised by huge emissions of CO₂ and CH₄ from the ground (Giammanco et al. 1998a). According to Bruno et al. (2001), soil gases at P39 are inferred to leak from a deep magma reservoir. Site VS is also located on the southwestern foot of Etna, just a few kilometres east of site P39. It is part of a large mud volcano (Vallone Salato, which is one of the three mud volcanoes locally known as "Salinelle", because they emit not only gas and mud, but also highly saline waters) that occupies an area of some hundred square metres. Lastly, site Naftia is a mofette that is today exploited for the production of industrial CO₂ (Mofeta dei Palici plant, CO₂ output estimated as about 200 tons/day, R. Romano pers. comm.) and is located about 40 km SW of Mt. Etna near the city of Palagonia. The last 3 sites are close to a major NE-SW fault system that probably runs across eastern Sicily and passes through Etna (Bosquet et al. 1988; Gurrieri et al. 1998). This fault system would also correspond to one of the main directions of magma rise beneath Etna (Rasa et al. 1995).

The collected gas samples were analysed in the lab for the determination of CO₂, He, H₂, O₂, N₂, CH₄ and CO concentrations, together with the isotopic ratios of carbon ($\delta^{13}\text{C}$) and oxygen ($\delta^{18}\text{O}$) of CO₂ and He (R/Ra). Samples of fumarole and soil gases were collected at a depth of 50 cm through steel tubes connected to a syringe and were then stored into glass flasks equipped with vacuum stopcocks. Upon collection, samples for carbon isotopes analyses were first passed through a tube containing lead acetate in order to eliminate H₂S and water vapour. Chemical analyses were done by using a Perkin Elmer 8500 gas chromatograph with argon as carrier gas and equipped with a 4 m Carbosieve S II column. In order to evaluate the concentration of He, H₂, O₂, N₂ and CO₂ a TCD detector was used, while CH₄ and CO concentrations were determined using a FID detector coupled with a methanizer. The detection limits were about 6 ppm vol. for He, 2 ppm vol. for H₂, 1 ppm vol. for CO, 2 ppm vol. for CH₄, 0.05% vol. for O₂ and 0.1% vol. for N₂. Analyses of carbon and oxygen isotopes of CO₂ were carried out by using a Finnigan Delta plus mass spectrometer. Values of carbon isotope of CO₂ are expressed in $\delta\text{‰}$ vs. PBD, accuracy being 0.1 $\delta\text{‰}$. Values of oxygen isotopes of CO₂ are expressed in $\delta\text{‰}$ vs V-SMOW, accuracy being 0.2 $\delta\text{‰}$. The ³He/⁴He ratios were measured by a double collector VG Masstorr FX (error $\pm 1\%$) and the ⁴He/²⁰Ne ratio by a quadruple mass spectrometer VG Masstorr FX (accuracy $\pm 5\%$). Soil CO₂ emissions were determined using the "dynamic concentration" method of Gurrieri and Valenza (1988), also described in Giammanco et al. (1995).

The analytical results for all the collected gas samples are shown in Table 1.

Table. 1. Chemical and isotopic composition of the sampled points. Analytical data are expressed as %vol (CO₂, N₂, O₂) and ppmvol (He, H₂, CO, CH₄), dynamic concentration of CO₂ as ppmvol.

samples	date	He	H ₂	O ₂	N ₂	CO	CH ₄	CO ₂	δ ¹³ C _{CO2}	He R/Ra	CO ₂ dyn	T°C
BLV	6.7.00	8.39	110.0	14.97	71.6	b.d.l.	44.8	14.7	n.d.	1.58	40000	87.5
	3.8.00	3.43	17.8	14.70	76.1	b.d.l.	36.2	10.3	-1.40	1.56	68000	87.3
	30.8.00	7.14	293.0	16.90	67.9	1.40	47.1	12.3	-1.55	1.56	74200	87.0
	14.9.00	b.d.l.	114.2	17.48	72.7	b.d.l.	24.4	9.9	-1.23	1.50	58500	89.8
	18.10.00	3.06	171.0	16.97	74.5	1.84	29.0	9.3	-1.31	1.60	56000	88.0
	8.11.00	b.d.l.	98.0	19.50	74.7	1.25	23.7	7.2	-2.18	1.42	41000	88.0
	7.12.00	b.d.l.	28.8	17.70	74.1	b.d.l.	29.1	9.2	-1.15	1.54	55200	88.4
	19.12.00	4.08	23.7	18.50	74.7	b.d.l.	30.4	8.0	n.d.	1.29	51500	86.1
	11.1.01	3.96	18.1	18.73	76.5	b.d.l.	22.2	6.1	-2.89	1.36	36000	86.3
	23.1.01	b.d.l.	125.6	19.00	75.5	b.d.l.	18.8	5.0	-0.97	1.31	34000	86.0
	10.2.01	4.44	126.0	17.46	72.9	b.d.l.	27.6	9.6	-1.41	1.49	56000	86.5
	22.3.01	8.30	178.6	18.90	76.5	b.d.l.	25.7	1.1	-1.13	1.33	42000	85.8
	11.4.01	b.d.l.	80.0	17.90	71.3	b.d.l.	48.0	11.0	-1.16	1.63	65100	84.8
	4.5.01	b.d.l.	136.3	16.64	71.0	b.d.l.	46.2	13.5	-0.75	1.73	70000	87.0
	17.5.01	b.d.l.	62.0	18.20	76.1	b.d.l.	25.1	6.0	-1.49	1.42	38300	87.7
	5.6.01	4.56	173.0	18.11	73.7	b.d.l.	34.0	8.6	-1.19	1.50	50700	85.5
	29.6.01	b.d.l.	325.0	15.06	73.3	3.50	30.8	12.4	-1.04	1.76	70300	86.6
	12.7.01	5.67	476.0	16.18	68.8	3.52	54.0	15.6	-0.82	1.95	n.d.	91.3
	17.7.01	1.58	271.0	15.24	66.9	b.d.l.	57.7	18.5	-1.38	n.d.	11000	88.9
	20.2.02	9.06	125.9	12.62	55.2	1.18	89.0	32.6	-1.35	n.d.	172000	88.7
	20.3.02	2.62	212.8	14.70	62.4	6.60	61.4	23.7	-1.45	n.d.	130000	88.4
	18.4.02	9.59	145.7	13.16	59.2	116.81	54.7	28.1	-1.59	n.d.	139000	88.8
	5.7.02	b.d.l.	195.2	13.27	58.1	7.44	89.0	28.8	-1.53	n.d.	145000	88.3
	23.7.02	b.d.l.	78.1	13.64	61.6	5.07	87.9	24.9	-1.37	n.d.	144000	87.4
	2.8.02	b.d.l.	148.7	13.93	61.7	7.37	58.2	24.6	-1.78	n.d.	124000	88.4
	17.9.02	b.d.l.	120.1	14.44	62.2	7.45	64.1	23.4	-1.60	n.d.	n.d.	n.d.
	22.10.02	b.d.l.	76.9	14.04	63.1	4.19	53.9	22.9	-1.19	n.d.	120000	88.1
	15.11.02	b.d.l.	51.1	17.89	71.9	5.29	25.8	10.4	-2.20	n.d.	76000	86.1
	9.5.03	6.05	31.5	13.75	57.9	112.89	39.2	28.5	-1.86	n.d.	153000	84.8
	18.6.03	b.d.l.	23.9	18.16	70.6	3.24	17.2	11.5	-1.89	n.d.	156000	105.0
	17.7.03	b.d.l.	24.1	14.28	63.8	33.10	29.1	21.9	-1.62	n.d.	125000	86.5
	TDF	6.7.00	b.d.l.	b.d.l.	19.8	76.9	b.d.l.	2.2	3.8	-1.97	1.58	20000
3.8.00		2.36	b.d.l.	18.6	n.d.	b.d.l.	2.7	2.5	-2.83	1.35	19200	17.2
30.8.00		b.d.l.	5.1	23.0	70.5	b.d.l.	5.4	0.9	-3.79	1.28	18000	25.0
15.9.00		b.d.l.	b.d.l.	20.4	76.4	b.d.l.	2.1	3.7	-1.14	1.46	20000	16.1
18.10.00		4.09	b.d.l.	20.0	76.8	1.8	3.4	2.8	-2.25	1.45	16800	11.4
8.11.00		n.d.	n.d.	n.d.	n.d.	n.d.	n.d.	n.d.	n.d.	1.42	n.d.	5.0
5.12.00		n.d.	n.d.	n.d.	n.d.	n.d.	n.d.	n.d.	n.d.	1.54	n.d.	n.d.
19.12.00		3.63	b.d.l.	20.9	78.1	b.d.l.	3.4	0.8	-3.80	1.18	7200	n.d.
9.2.01		4.50	b.d.l.	20.2	77.6	b.d.l.	4.6	2.6	-2.67	1.39	16000	8.7
12.4.01		b.d.l.	b.d.l.	20.2	77.4	b.d.l.		2.3	-2.31	1.30	9800	6.5
4.5.01		b.d.l.	b.d.l.	20.4	76.6	b.d.l.	34.7	3.1	-2.48	1.49	15700	12.5
17.5.01		n.d.	n.d.	n.d.	n.d.	n.d.	n.d.	n.d.	n.d.	1.42	n.d.	14.6
5.6.01		n.d.	n.d.	n.d.	n.d.	n.d.	n.d.	n.d.	n.d.	1.50	n.d.	13.1
28.6.01		n.d.	n.d.	n.d.	n.d.	n.d.	n.d.	n.d.	n.d.	1.76	600	14.6
12.7.01		n.d.	n.d.	n.d.	n.d.	n.d.	n.d.	n.d.	n.d.	1.95	n.d.	19.3
14.9.01		n.d.	n.d.	n.d.	n.d.	n.d.	n.d.	n.d.	n.d.	n.d.	n.d.	14.9
2.10.01		n.d.	n.d.	n.d.	n.d.	n.d.	n.d.	n.d.	n.d.	n.d.	n.d.	17.3
25.10.01		b.d.l.	b.d.l.	21.4	78.0	b.d.l.	b.d.l.	0.7	-1.41	n.d.	6000	13.6

Table. 1. Continued.

samples	date	He	H ₂	O ₂	N ₂	O ₃	CH ₄	CO ₂	$\delta^{13}\text{C}_{\text{CO}_2}$	He R/Ra	CO ₂ dyn	T°C	
TDF	29.10.01	n.d.	n.d.	n.d.	n.d.	b.d.l.	n.d.	n.d.	-1.57	n.d.	17000	15.0	
	6.11.01	7.02	b.d.l.	19.6	75.7	b.d.l.	38.4	4.7	-1.41	n.d.	27000	16.1	
	6.12.01	n.d.	n.d.	n.d.	n.d.	n.d.	n.d.	n.d.	n.d.	n.d.	12000	5.7	
	22.1.02	b.d.l.	4.7	20.1	74.9	b.d.l.	14.8	4.8	b.d.l.	n.d.	30000	5.7	
	20.2.02	b.d.l.	b.d.l.	20.0	75.3	b.d.l.	10.2	4.8	b.d.l.	n.d.	27000	n.d.	
	18.4.02	b.d.l.	b.d.l.	20.2	75.9	29.7	0.0	4.0	-3.47	n.d.	18000	7.1	
	16.5.02	b.d.l.	b.d.l.	20.8	73.5	21.0	11.6	6.0	-1.45	n.d.	39000	10.1	
	30.5.02	b.d.l.	b.d.l.	20.2	75.3	14.1	3.6	4.6	-2.44	n.d.	13000	16.9	
	25.6.02	b.d.l.	b.d.l.	20.3	75.1	11.2	43.0	4.7	-2.39	n.d.	n.d.	n.d.	
	1.8.02	b.d.l.	b.d.l.	20.2	73.8	8.6	26.6	6.4	-2.96	n.d.	32400	16.0	
	9.5.03	b.d.l.	39.3	18.4	73.1	162.9	38.9	8.6	n.d.	n.d.	53000	52.6	
	18.6.03	b.d.l.	b.d.l.	21.5	78.5	4.7	5.9	0.2	-7.57	n.d.	n.d.	n.d.	
	samples	date	He	H ₂	O ₂	N ₂	CO	CH ₄	CO ₂	$\delta^{13}\text{C}_{\text{CO}_2}$	He R/Ra	CO ₂ dyn	T°C
	RNE	15.9.00	b.d.l.	b.d.l.	18.80	72.75	b.d.l.	293.0	8.6	-3.79	1.85	80000	42.0
18.10.00		b.d.l.	b.d.l.	19.91	76.00	b.d.l.	122.7	4.2	-3.91	1.55	20000	37.3	
8.11.00		2.39	b.d.l.	20.09	75.45	b.d.l.	285.0	6.0	-3.92	1.43	40000	42.0	
19.12.00		b.d.l.	b.d.l.	18.81	73.70	b.d.l.	144.0	8.1	-3.37	1.45	40000	35.0	
3.5.01		b.d.l.	b.d.l.	17.70	70.80	b.d.l.	1011	13.1	-3.26	2.43	92500	47.5	
17.5.01		b.d.l.	b.d.l.	20.49	77.07	b.d.l.	19.6	2.3	-3.73	1.21	15300	40.8	
5.6.01		b.d.l.	b.d.l.	20.91	77.07	3.78	21.0	3.1	n.d.	1.29	19600	35.6	
28.6.01		b.d.l.	b.d.l.	19.21	73.65	1.91	71.8	8.0	-3.43	1.81	36000	38.1	
12.7.01		b.d.l.	b.d.l.	23.66	78.00	b.d.l.	161.3	5.1	-3.52	1.42	n.d.	34.3	
17.7.01		b.d.l.	b.d.l.	19.46	75.62	b.d.l.	41.9	8.1	-3.83	n.d.	18000	37.4	
21.7.01		9.48	b.d.l.	19.80	76.17	b.d.l.	143.0	4.0	-2.65	1.43	27500	33.9	
30.8.01		b.d.l.	b.d.l.	19.30	76.40	2.84	252.4	4.0	-4.23	n.d.	20000	35.5	
20.9.01		2.91	b.d.l.	20.47	77.20	b.d.l.	148.0	2.9	-4.18	n.d.	14000	29.2	
9.10.01		5.02	b.d.l.	19.50	75.10	2.50	207.0	6.1	-3.53	n.d.	32300	31.9	
25.10.01		b.d.l.	b.d.l.	21.00	77.80	b.d.l.	b.d.l.	1.8	-2.86	n.d.	27000	36.7	
29.10.01		b.d.l.	n.d.	n.d.	n.d.	n.d.	n.d.	n.d.	-2.01	n.d.	24000	31.0	
6.11.01		b.d.l.	31.34	19.10	74.45	74.70	135.6	6.6	n.d.	n.d.	40500	44.6	
22.11.01		n.d.	n.d.	n.d.	n.d.	n.d.	n.d.	n.d.	-3.69	n.d.	20000	46.2	
17.4.02		b.d.l.	b.d.l.	18.10	71.45	24.77	1072	10.40	-3.95	n.d.	46000	50.9	
16.5.02		b.d.l.	b.d.l.	18.80	73.63	11.13	791.4	7.67	-3.45	n.d.	52500	48.2	
31.5.02		b.d.l.	b.d.l.	19.29	72.95	11.56	263.3	7.91	-3.86	n.d.	n.d.	30.3	
25.6.02		b.d.l.	b.d.l.	19.65	74.62	9.20	344.5	5.76	-3.90	n.d.	15000	40.1	
24.7.02		b.d.l.	b.d.l.	20.28	77.68	9.45	55.3	2.03	-4.36	n.d.	7600	30.4	
1.8.02		b.d.l.	b.d.l.	20.58	77.35	7.67	114.4	2.15	-4.20	n.d.	14000	33.0	
19.9.02		b.d.l.	b.d.l.	20.13	77.55	8.20	30.9	2.42	n.c.	n.d.	n.d.	35.4	
22.10.02		b.d.l.	b.d.l.	20.63	77.04	4.70	15.5	2.58	-3.47	n.d.	17000	33.6	
21.5.03		b.d.l.	b.d.l.	16.20	66.72	25.56	1336	17.10	-3.97	n.d.	130000	44.4	
27.6.03	b.d.l.	b.d.l.	20.50	76.30	16.14	221.5	3.96	n.d.	n.d.	27000	39.0		
16/703	b.d.l.	b.d.l.	20.77	77.76	17.10	166.7	1.54	-3.56	n.d.	15000	40.8		
samples	date	He	H ₂	O ₂	N ₂	CO	CH ₄	CO ₂	$\delta^{13}\text{C}_{\text{CO}_2}$	He R/Ra	CO ₂ dyn	T°C	
P78	15.9.00	b.d.l.	b.d.l.	17.2	76.18	2.5	17.9	7.1	-9.69	1.15	24439	n.d.	
	4.10.00	3.9	b.d.l.	17.0	76.50	b.d.l.	b.d.l.	6.5	-11.81	1.30	36511	n.d.	
	18.10.00	b.d.l.	b.d.l.	20.4	77.60	b.d.l.	4.4	1.1	-10.61	1.06	9750	n.d.	
	8.11.00	b.d.l.	b.d.l.	18.7	73.97	b.d.l.	b.d.l.	7.4	-6.49	1.24	23100	n.d.	
	5.12.00	b.d.l.	b.d.l.	20.9	77.75	b.d.l.	36.1	0.3	-9.18	1.02	2800	n.d.	

Table. 1. Continued.

samples	date	He	H ₂	O ₂	N ₂	CO	CH ₄	CO ₂	$\delta^{13}\text{C}_{\text{CO}_2}$	He R/Ra	CO ₂ dyn	T°C
P78	18.12.00	b.d.l.	b.d.l.	20.8	77.80	b.d.l.	b.d.l.	n.d.	n.d.	n.d.	550	n.d.
	10.1.01	n.d.	n.d.	n.d.	n.d.	n.d.	n.d.	n.d.	-19.55	n.d.	400	n.d.
	22.1.01	n.d.	n.d.	n.d.	n.d.	n.d.	n.d.	n.d.	n.d.	n.d.	2600	n.d.
	9.2.01	b.d.l.	b.d.l.	20.0	78.20	b.d.l.	b.d.l.	1.6	-2.05	n.d.	7500	n.d.
	27.2.01	n.d.	n.d.	n.d.	n.d.	n.d.	n.d.	n.d.	n.d.	n.d.	1700	n.d.
	22.3.01	b.d.l.	b.d.l.	19.9	75.01	b.d.l.	23.7	6.9	-14.65	1.08	34000	n.d.
	11.4.01	b.d.l.	b.d.l.	18.0	77.80	b.d.l.	b.d.l.	4.3	-11.66	1.10	n.d.	n.d.
	4.5.01	b.d.l.	b.d.l.	20.2	76.07	b.d.l.	34.4	4.4	-5.93	1.12	24000	n.d.
	16.5.01	b.d.l.	b.d.l.	18.1	76.08	b.d.l.	27.4	6.4	-8.31	1.18	63000	n.d.
	5.6.01	b.d.l.	b.d.l.	19.8	75.64	b.d.l.	12.5	5.4	-6.51	1.18	43000	n.d.
	28.6.01	b.d.l.	b.d.l.	19.0	73.89	4.5	b.d.l.	7.8	-5.08	1.35	67000	n.d.
	12.7.01	b.d.l.	b.d.l.	20.2	74.80	b.d.l.	b.d.l.	7.5	-4.82	1.28	62000	n.d.
	17.7.01	b.d.l.	b.d.l.	18.9	76.23	b.d.l.	b.d.l.	5.8	-5.87	n.d.	63300	n.d.
	21.7.01	b.d.l.	b.d.l.	19.0	76.07	b.d.l.	b.d.l.	6.5	-6.23	1.24	63500	n.d.
	24.7.01	b.d.l.	b.d.l.	18.9	74.04	5.5	b.d.l.	7.1	-6.43	1.79	63000	n.d.
	27.7.01	b.d.l.	b.d.l.	19.0	74.58	b.d.l.	b.d.l.	6.3	-6.13	n.d.	n.d.	n.d.
	31.7.01	4.6	b.d.l.	18.9	74.13	3.3	21.8	6.7	-5.59	n.d.	n.d.	n.d.
	3.8.01	b.d.l.	b.d.l.	18.7	74.80	b.d.l.	b.d.l.	6.4	n.d.	n.d.	63500	n.d.
	7.8.01	b.d.l.	b.d.l.	18.7	75.20	9.1	b.d.l.	6.6	-5.52	n.d.	62200	n.d.
	10.8.01	b.d.l.	b.d.l.	19.2	76.06	1.0	b.d.l.	6.3	-4.97	n.d.	n.d.	n.d.
	13.8.01	b.d.l.	b.d.l.	19.1	75.32	8.5	28.8	6.5	-6.73	n.d.	n.d.	n.d.
	16.8.01	b.d.l.	b.d.l.	19.3	76.01	12.2	8.2	6.4	-6.14	n.d.	n.d.	n.d.
	24.8.01	b.d.l.	b.d.l.	n.d.	n.d.	n.d.	n.d.	n.d.	-6.69	n.d.	n.d.	n.d.
	31.8.01	b.d.l.	b.d.l.	18.6	75.10	1.2	59.8	6.2	-6.14	n.d.	61100	n.d.
	7.9.01	b.d.l.	b.d.l.	19.0	75.34	5.7	88.0	6.5	-5.98	n.d.	57200	n.d.
	14.9.01	b.d.l.	b.d.l.	18.2	72.30	b.d.l.	b.d.l.	6.8	-5.73	n.d.	n.d.	n.d.
	18.9.01	b.d.l.	b.d.l.	19.7	75.34	b.d.l.	265.0	3.8	-6.74	n.d.	n.d.	n.d.
	20.9.01	b.d.l.	b.d.l.	19.4	74.38	b.d.l.	b.d.l.	7.2	-5.97	n.d.	59000	n.d.
	25.9.01	b.d.l.	b.d.l.	19.4	74.26	3.4	b.d.l.	7.1	-5.33	n.d.	n.d.	n.d.
	2.10.01	6.5	b.d.l.	19.5	75.00	b.d.l.	b.d.l.	5.6	-4.71	n.d.	n.d.	n.d.
	9.10.01	5.0	b.d.l.	18.0	73.70	b.d.l.	67.6	8.1	-5.58	n.d.	71536	n.d.
	18.10.01	4.1	b.d.l.	20.1	77.80	b.d.l.	b.d.l.	3.0	n.d.	n.d.	n.d.	n.d.
	25.10.01	n.d.	n.d.	n.d.	n.d.	n.d.	n.d.	n.d.	-4.15	n.d.	63500	n.d.
	29.10.01	n.d.	n.d.	n.d.	n.d.	n.d.	n.d.	n.d.	-3.80	n.d.	20000	n.d.
	6.11.01	n.d.	n.d.	n.d.	n.d.	n.d.	n.d.	n.d.	-5.59	n.d.	49000	n.d.
	13.11.01	b.d.l.	b.d.l.	22.0	77.74	b.d.l.	b.d.l.	1.1	n.d.	n.d.	n.d.	n.d.
	21.11.01	b.d.l.	20.97	21.5	78.41	43.0	b.d.l.	0.2	-0.39	n.d.	51500	n.d.
	23.11.01	n.d.	n.d.	n.d.	n.d.	n.d.	n.d.	n.d.	-2.42	n.d.	n.d.	n.d.
	5.12.01	n.d.	n.d.	n.d.	n.d.	n.d.	n.d.	n.d.	-6.97	n.d.	12000	n.d.
	9.1.02	b.d.l.	b.d.l.	21.3	78.60	1.0	5.3	0.55	n.d.	n.d.	2100	n.d.
	22.1.02	4.0	b.d.l.	20.8	78.55	1.0	n.d.	0.53	-14.33	n.d.	4500	n.d.
	20.2.02	b.d.l.	b.d.l.	20.0	79.15	1.0	4.0	0.94	-14.93	n.d.	4800	n.d.
	4.3.02	b.d.l.	b.d.l.	19.8	78.51	1.0	n.d.	2.25	-19.49	n.d.	26922	n.d.
	19.3.02	2.0	b.d.l.	20.7	78.47	7.1	35.1	0.90	-16.82	n.d.	3400	n.d.
	4.4.02	b.d.l.	b.d.l.	20.2	79.58	53.0	0.1	0.48	n.d.	n.d.	2100	n.d.
	17.4.02	b.d.l.	b.d.l.	20.7	79.40	n.d.	n.d.	0.03	-19.26	n.d.	2000	n.d.
	3.5.02	b.d.l.	b.d.l.	19.2	78.59	12.0	n.d.	2.44	-18.11	n.d.	18000	n.d.
	14.5.02	b.d.l.	b.d.l.	19.4	79.44	19.3	n.d.	1.02	-16.18	n.d.	3900	n.d.
	31.5.02	b.d.l.	b.d.l.	19.6	77.09	9.3	n.d.	3.71	-12.11	n.d.	n.d.	n.d.
	24.6.02	b.d.l.	b.d.l.	19.8	73.59	8.7	128.7	6.59	-6.76	n.d.	13000	n.d.
	23.7.02	b.d.l.	b.d.l.	19.5	74.80	7.4	n.d.	5.86	-6.23	n.d.	47590	n.d.
	1.8.02	b.d.l.	b.d.l.	19.1	74.89	6.8	n.d.	6.01	-6.28	n.d.	35000	n.d.

Table. 1. Continued.

samples	date	He	H ₂	O ₂	N ₂	CO	CH ₄	CO ₂	$\delta^{13}\text{C}_{\text{CO}_2}$	He R/Ra	CO ₂ dyn	T°C	
P78	17.9.02	b.d.l.	b.d.l.	18.2	75.58	6.5	n.d.	6.29	-6.70	n.d.	38460	n.d.	
	21.10.02	b.d.l.	b.d.l.	19.7	75.50	4.8	n.d.	5.69	-6.19	n.d.	14500	n.d.	
	28.10.02	b.d.l.	b.d.l.	18.8	74.88	7.7	n.d.	6.88	-4.08	n.d.	61500	n.d.	
	29.10.02	b.d.l.	b.d.l.	20.7	77.88	5.29	n.d.	1.52	-2.79	n.d.	n.d.	n.d.	
	31.10.02	b.d.l.	b.d.l.	19.0	74.94	12.5	7.5	6.37	-5.03	n.d.	48500	n.d.	
	2.11.02	b.d.l.	b.d.l.	19.0	76.04	8.8	8.3	5.01	-6.78	n.d.	n.d.	n.d.	
	7.11.02	b.d.l.	b.d.l.	19.3	76.09	4.3	n.d.	4.67	-7.19	n.d.	46150	n.d.	
	15.11.02	b.d.l.	b.d.l.	20.4	77.97	6.6	4.5	1.31	-13.42	n.d.	42000	n.d.	
	22.11.02	b.d.l.	b.d.l.	21.0	78.79	5.8	n.d.	0.16	-15.26	n.d.	7500	n.d.	
	28.11.02	n.d.	n.d.	n.d.	n.d.	n.d.	n.d.	n.d.	n.d.	n.d.	1000	n.d.	
	4.12.02	b.d.l.	b.d.l.	20.8	78.40	6.8	1.3	0.91	-14.05	n.d.	17200	n.d.	
	11.12.02	n.d.	n.d.	n.d.	n.d.	n.d.	n.d.	n.d.	n.d.	n.d.	400	n.d.	
	18.12.02	b.d.l.	b.d.l.	18.9	78.20	3.0	n.d.	2.93	-18.86	n.d.	9500	n.d.	
	14.1.03	n.d.	n.d.	n.d.	n.d.	n.d.	n.d.	n.d.	n.d.	n.d.	4200	n.d.	
	28.1.03	b.d.l.	b.d.l.	21.0	78.84	4.9	n.d.	0.22	n.d.	n.d.	5000	n.d.	
	19.2.03	n.d.	n.d.	n.d.	n.d.	n.d.	n.d.	n.d.	n.d.	n.d.	150	n.d.	
	13.3.03	b.d.l.	b.d.l.	20.5	78.87	5.4	n.d.	1.07	-19.47	n.d.	9000	n.d.	
	15.4.03	b.d.l.	32.20	19.7	79.93	146.1	17.1	0.43	-21.68	n.d.	3000	n.d.	
	18.4.03	n.d.	n.d.	n.d.	n.d.	n.d.	n.d.	n.d.	n.d.	n.d.	10500	n.d.	
	8.5.03	b.d.l.	3.00	19.0	76.10	114.1	7.7	4.90	n.d.	n.d.	50000	n.d.	
	17.6.03	b.d.l.	b.d.l.	19.0	73.96	28.6	103.4	6.97	-6.30	n.d.	47690	n.d.	
	26.6.03	n.d.	n.d.	n.d.	n.d.	n.d.	n.d.	n.d.	n.d.	n.d.	66150	n.d.	
	16.7.03	b.d.l.	b.d.l.	18.6	72.81	14.2	b.d.l.	8.60	-7.40	n.d.	80800	n.d.	
	samples	date	He	H ₂	O ₂	N ₂	CO	CH ₄	CO ₂	$\delta^{13}\text{C}_{\text{CO}_2}$	He R/Ra	CO ₂ dyn	T°C
	Naftia	31.7.00	n.d.	n.d.	n.d.	n.d.	n.d.	n.d.	n.d.	-0.90	6.22	n.d.	n.d.
		15.9.00	87.8	b.d.l.	0.037	0.55	b.d.l.	4653	99.7	-1.00	6.19	n.d.	n.d.
3.10.00		92.3	b.d.l.	0.099	0.76	b.d.l.	5523	99.6	-0.95	6.61	n.d.	n.d.	
18.10.00		88.0	b.d.l.	0.058	0.49	b.d.l.	4883	99.1	-0.93	6.64	n.d.	n.d.	
7.11.00		89.2	b.d.l.	b.d.l.	0.47	b.d.l.	4878	99.1	-1.41	6.51	n.d.	n.d.	
5.12.00		89.7	b.d.l.	0.012	0.50	b.d.l.	5000	99.6	-1.39	6.45	n.d.	n.d.	
19.12.00		n.d.	n.d.	n.d.	n.d.	n.d.	n.d.	n.d.	-1.71	6.55	n.d.	n.d.	
11.1.01		108.5	b.d.l.	0.034	0.51	b.d.l.	5900	99.0	-1.01	6.27	n.d.	n.d.	
22.1.01		n.d.	n.d.	n.d.	n.d.	n.d.	n.d.	n.d.	-0.99	6.52	n.d.	n.d.	
10.2.01		94.7	b.d.l.	b.d.l.	0.46	b.d.l.	4652	99.0	-0.98	6.30	n.d.	n.d.	
27.2.01		65.0	b.d.l.	0.060	0.51	b.d.l.	4473	98.4	-0.99	6.26	n.d.	n.d.	
22.3.01		115.5	b.d.l.	b.d.l.	0.42	b.d.l.	5200	97.4	-0.98	6.36	n.d.	n.d.	
11.4.01		86.0	b.d.l.	b.d.l.	0.42	b.d.l.	4560	99.3	-1.05	6.37	n.d.	n.d.	
3.5.01		85.6	b.d.l.	b.d.l.	0.39	b.d.l.	4925	98.9	-0.97	6.50	n.d.	n.d.	
17.5.01		78.0	b.d.l.	b.d.l.	0.46	b.d.l.	5091	99.0	-0.92	6.50	n.d.	n.d.	
6.6.01		105.0	b.d.l.	b.d.l.	0.42	b.d.l.	5100	99.2	-0.97	6.36	n.d.	n.d.	
28.6.01		94.1	b.d.l.	b.d.l.	0.45	b.d.l.	4833	99.1	-0.97	6.44	n.d.	n.d.	
12.7.01		87.8	b.d.l.	b.d.l.	0.420	b.d.l.	4913	97.3	-0.91	6.65	n.d.	n.d.	
24.7.01		97.5	b.d.l.	b.d.l.	0.52	b.d.l.	5005	99.0	-0.97	6.83	n.d.	n.d.	
27.7.01		102.2	b.d.l.	b.d.l.	0.54	b.d.l.	5100	99.1	-0.97	7.13	n.d.	n.d.	
31.7.01		63.6	b.d.l.	0.330	1.02	b.d.l.	5068	98.1	-0.96	6.84	n.d.	n.d.	
3.8.01		51.0	b.d.l.	b.d.l.	0.53	b.d.l.	5117	99.3	-0.99	6.87	n.d.	n.d.	
7.8.01		88.9	b.d.l.	b.d.l.	0.50	b.d.l.	5061	100.0	-1.00	6.39	n.d.	n.d.	
10.8.01	n.d.	n.d.	n.d.	n.d.	n.d.	n.d.	n.d.	-1.05	6.53	n.d.	n.d.		
13.8.01	120.5	b.d.l.	b.d.l.	0.57	b.d.l.	5600	99.2	-1.02	6.56	n.d.	n.d.		
16.8.01	121.0	b.d.l.	b.d.l.	0.56	b.d.l.	5600	98.8	-0.62	6.49	n.d.	n.d.		

Table. 1. Continued.

samples	date	He	H ₂	O ₂	N ₂	CO	CH ₄	CO ₂	$\delta^{13}\text{C}_{\text{CO}_2}$	He R/Ra	CO ₂ dyn	T°C
Naftia	24.8.01	n.d.	n.d.	n.d.	n.d.	n.d.	n.d.	n.d.	-1.03	6.48	n.d.	n.d.
	31.8.01	86.7	b.d.l.	b.d.l.	0.54	b.d.l.	5700	99.0	-1.12	6.52	n.d.	n.d.
	7.9.01	126.0	b.d.l.	b.d.l.	0.54	b.d.l.	5720	99.0	-1.07	6.48	n.d.	n.d.
	14.9.01	90.8	b.d.l.	b.d.l.	0.42	b.d.l.	5500	97.8	-1.10	6.40	n.d.	n.d.
	18.9.01	118.2	b.d.l.	b.d.l.	0.50	b.d.l.	4500	97.8	-1.05	6.46	n.d.	n.d.
	25.9.01	85.6	b.d.l.	b.d.l.	0.23	b.d.l.	6000	99.4	-1.03	6.50	n.d.	n.d.
	2.10.01	88.3	b.d.l.	b.d.l.	0.15	b.d.l.	5800	99.5	-1.06	n.d.	n.d.	n.d.
	9.10.01	112.0	b.d.l.	b.d.l.	0.54	b.d.l.	6300	99.9	-1.03	6.40	n.d.	n.d.
	16.10.01	93.7	b.d.l.	b.d.l.	0.50	b.d.l.	5300	99.0	-1.03	6.38	n.d.	n.d.
	23.10.01	n.d.	n.d.	n.d.	n.d.	n.d.	n.d.	n.d.	-1.04	6.49	n.d.	n.d.
	30.10.01	n.d.	n.d.	n.d.	n.d.	n.d.	n.d.	n.d.	-0.92	6.67	n.d.	n.d.
	7.11.01	102.4	b.d.l.	b.d.l.	0.52	2.13	5100	99.0	-0.74	n.d.	n.d.	n.d.
	13.11.01	n.d.	n.d.	n.d.	n.d.	n.d.	n.d.	n.d.	-1.00	n.d.	n.d.	n.d.
	21.11.01	88.5	b.d.l.	b.d.l.	0.47	b.d.l.	5369	99.4	-0.86	6.72	n.d.	n.d.
	27.11.01	86.6	b.d.l.	b.d.l.	0.48	b.d.l.	5460	98.9	-0.95	6.60	n.d.	n.d.
	5.12.01	93.5	b.d.l.	b.d.l.	0.46	b.d.l.	5475	98.9	-0.99	n.d.	n.d.	n.d.
	11.12.01	107.6	b.d.l.	b.d.l.	0.45	2.9	5292	98.8	-1.05	6.59	n.d.	n.d.
	20.12.01	110.0	b.d.l.	b.d.l.	0.49	b.d.l.	5779	99.0	n.d.	n.d.	n.d.	n.d.
	28.12.01	122.7	b.d.l.	b.d.l.	0.55	b.d.l.	6531	98.8	n.d.	n.d.	n.d.	n.d.
	9.1.02	119.2	b.d.l.	b.d.l.	0.48	b.d.l.	5500	98.87	n.d.	6.55	n.d.	n.d.
	22.1.02	137.7	b.d.l.	b.d.l.	0.60	1.33	6600	98.8	-1.00	6.55	n.d.	n.d.
	5.2.02	78.4	b.d.l.	b.d.l.	0.49	b.d.l.	4800	98.8	-1.03	6.64	n.d.	n.d.
	12.3.02	103.1	b.d.l.	b.d.l.	0.46	b.d.l.	4600	96.9	-1.00	6.41	n.d.	n.d.
	26.3.02	84.9	b.d.l.	b.d.l.	0.04	4.57	5500	99.7	-0.98	6.28	n.d.	n.d.
	9.4.02	120.0	b.d.l.	b.d.l.	0.53	b.d.l.	5440	99.2	-0.96	6.39	n.d.	n.d.
	23.4.02	n.d.	n.d.	n.d.	n.d.	n.d.	n.d.	n.d.	n.d.	6.13	n.d.	n.d.
	7.5.02	86.6	b.d.l.	b.d.l.	0.32	b.d.l.	6900	99.0	-0.98	6.45	n.d.	n.d.
	21.5.02	120.3	b.d.l.	b.d.l.	0.54	b.d.l.	5104	99.0	-0.97	6.37	n.d.	n.d.
	4.6.02	109.9	b.d.l.	b.d.l.	0.55	b.d.l.	5675	98.9	-0.98	6.39	n.d.	n.d.
	17.6.02	103.9	b.d.l.	b.d.l.	0.53	b.d.l.	5736	98.9	-0.97	6.46	n.d.	n.d.
	1.7.02	125.3	b.d.l.	b.d.l.	0.51	b.d.l.	5200	99.0	-0.98	6.16	n.d.	n.d.
	16.7.02	115.9	b.d.l.	b.d.l.	0.53	b.d.l.	5762	99.0	-1.00	6.18	n.d.	n.d.
	31.7.02	121.0	b.d.l.	1.490	5.72	b.d.l.	4854	92.4	-0.99	6.17	n.d.	n.d.
	4.8.02	n.d.	n.d.	n.d.	n.d.	n.d.	n.d.	n.d.	n.d.	6.17	n.d.	n.d.
	13.8.02	128.4	b.d.l.	0.360	0.52	b.d.l.	5397	98.9	-0.96	6.27	n.d.	n.d.
	28.8.02	114.2	b.d.l.	0.470	0.52	2.48	5900	98.5	-0.97	6.45	n.d.	n.d.
	10.9.02	n.d.	n.d.	n.d.	n.d.	n.d.	n.d.	n.d.	-1.00	6.29	n.d.	n.d.
	24.9.02	131.0	b.d.l.	0.460	0.54	b.d.l.	5700	98.5	-0.93	6.34	n.d.	n.d.
	10.10.02	111.8	b.d.l.	0.350	0.45	1.72	5900	98.6	-1.01	6.36	n.d.	n.d.
	21.10.02	134.0	b.d.l.	0.470	0.50	b.d.l.	6000	98.6	-0.95	6.26	n.d.	n.d.
	27.10.02	137.9	b.d.l.	0.450	0.48	b.d.l.	5400	98.5	n.d.	6.38	n.d.	n.d.
	30.10.02	78.3	b.d.l.	0.460	0.50	b.d.l.	5490	98.6	-1.07	6.28	n.d.	n.d.
	4.11.02	114.9	b.d.l.	0.390	0.51	b.d.l.	5800	98.7	-0.97	6.29	n.d.	n.d.
	8.11.02	87.6	b.d.l.	0.410	0.47	b.d.l.	5700	98.6	-0.94	6.25	n.d.	n.d.
	11.11.02	109.8	b.d.l.	0.450	0.51	b.d.l.	6000	98.8	-1.05	6.27	n.d.	n.d.
	14.11.02	103.7	b.d.l.	0.260	0.45	b.d.l.	5466	98.8	-1.05	6.27	n.d.	n.d.
	18.11.02	88.3	b.d.l.	0.410	0.61	b.d.l.	5158	98.5	-1.04	6.19	n.d.	n.d.
	21.11.02	86.3	b.d.l.	0.410	0.48	b.d.l.	5404	98.7	-1.07	6.35	n.d.	n.d.
	25.11.02	111.3	b.d.l.	0.000	0.51	b.d.l.	5742	99.1	-1.08	6.32	n.d.	n.d.
	2.12.02	112.0	b.d.l.	0.470	0.50	b.d.l.	5900	99.3	-1.04	6.33	n.d.	n.d.
	11.12.02	109.7	b.d.l.	0.430	0.51	b.d.l.	5805	98.5	-1.04	6.50	n.d.	n.d.
	17.12.02	110.5	b.d.l.	0.520	0.76	b.d.l.	5302	98.2	-0.98	6.45	n.d.	n.d.

Table. 1. Continued.

samples	date	He	H ₂	O ₂	N ₂	CO	CH ₄	CO ₂	$\delta^{13}\text{C}_{\text{CO}_2}$	He R/Ra	CO ₂ dyn	T°C
Naftia	24.12.02	98.9	b.d.l.	0.200	0.44	b.d.l.	5478	98.8	-0.92	6.49	n.d.	n.d.
	27.12.02	90.8	b.d.l.	0.230	0.40	b.d.l.	5080	99.0	-1.01	6.46	n.d.	n.d.
	8.1.03	91.0	b.d.l.	0.860	2.79	b.d.l.	4880	96.2	-1.05	n.d.	n.d.	n.d.
	16.1.03	106.0	b.d.l.	0.280	0.44	b.d.l.	5800	98.9	-1.29	6.44	n.d.	n.d.
	23.1.03	84.9	b.d.l.	0.280	0.46	b.d.l.	5600	99.1	-0.97	6.44	n.d.	n.d.
	30.1.03	109.6	b.d.l.	0.250	0.41	b.d.l.	6400	98.7	-0.92	6.45	n.d.	n.d.
	6.2.03	84.7	b.d.l.	0.250	0.42	b.d.l.	5299	98.9	-1.02	6.38	n.d.	n.d.
	22.2.03	n.d.	n.d.	n.d.	n.d.	n.d.	n.d.	n.d.	n.d.	6.34	n.d.	n.d.
	12.3.03	110.0	b.d.l.	0.290	0.43	b.d.l.	5300	99.5	-0.93	6.27	n.d.	n.d.
	2.4.03	93.6	b.d.l.	0.250	0.43	b.d.l.	5900	98.8	-0.99	6.46	n.d.	n.d.
	16.4.03	97.6	b.d.l.	0.370	0.50	b.d.l.	5219	98.7	-0.98	6.43	n.d.	n.d.
	6.5.03	74.9	b.d.l.	0.210	0.47	7.47	5272	98.9	-0.92	6.49	n.d.	n.d.
	30.5.03	n.d.	n.d.	n.d.	n.d.	n.d.	n.d.	n.d.	-1.03	6.21	n.d.	n.d.
	13.6.03	n.d.	n.d.	n.d.	n.d.	n.d.	n.d.	n.d.	-1.02	6.27	n.d.	n.d.
	24.6.03	n.d.	n.d.	n.d.	n.d.	n.d.	n.d.	n.d.	-1.07	6.39	n.d.	n.d.
	17.7.03	77.0	b.d.l.	b.d.l.	0.38	b.d.l.	5378	99.2	-1.12	n.d.	n.d.	n.d.
	<hr/>											
samples	date	He	H ₂	O ₂	N ₂	CO	CH ₄	CO ₂	$\delta^{13}\text{C}_{\text{CO}_2}$	He R/Ra	CO ₂ dyn	T°C
P39	3.8.00	57.3	29.7	0.18	1.90	b.d.l.	130300	87.2	1.16	6.84	317432	n.d.
	30.8.00	55.5	20.0	5.20	19.90	b.d.l.	101000	67.8	0.91	7.17	n.d.	n.d.
	15.9.00	40.6	9.8	6.41	25.81	b.d.l.	84500	60.4	0.82	6.70	84721	n.d.
	3.10.00	55.1	5.7	3.25	13.00	b.d.l.	116200	75.5	0.93	7.37	103554	n.d.
	7.11.00	41.2	b.d.l.	7.67	28.50	b.d.l.	82600	56.8	0.54	7.08	n.d.	n.d.
	5.12.00	62.9	16.5	0.02	0.59	b.d.l.	134500	87.5	0.64	6.75	539808	n.d.
	19.12.00	86.6	5.4	0.08	0.69	b.d.l.	140600	86.1	0.61	7.25	583424	n.d.
	10.1.01	55.2	2.0	0.08	0.58	b.d.l.	137100	87.5	1.06	6.84	395604	n.d.
	22.1.01	64.0	2.0	0.08	0.58	b.d.l.	134400	85.5	1.05	7.16	n.d.	n.d.
	10.2.01	53.0	2.0	0.03	0.16	b.d.l.	131000	87.4	1.37	6.92	690395	n.d.
	22.2.01	53.7	2.0	0.08	0.62	b.d.l.	125200	87.5	0.90	6.87	598732	n.d.
	22.3.01	75.4	2.0	b.d.l.	0.53	b.d.l.	123700	88.3	1.00	6.99	575917	n.d.
	11.4.01	73.0	2.0	0.07	0.57	b.d.l.	130000	87.3	1.32	7.03	n.d.	n.d.
	2.5.01	63.3	2.0	0.06	0.75	b.d.l.	123700	87.8	1.24	6.96	450300	n.d.
	16.5.01	63.6	2.0	0.06	0.79	b.d.l.	124100	87.4	1.34	7.20	n.d.	n.d.
	5.6.01	70.8	2.0	0.09	1.19	b.d.l.	130000	86.8	1.40	6.97	n.d.	n.d.
	28.6.01	68.4	6.4	0.64	2.00	3.3	121200	86.9	1.48	7.11	n.d.	n.d.
	12.7.01	61.5	8.4	0.11	1.08	b.d.l.	125500	86.9	1.58	7.34	n.d.	n.d.
	17.7.01	62.9	7.5	2.31	6.33	b.d.l.	117700	83.3	1.33	7.37	n.d.	n.d.
	24.7.01	81.8	19.7	0.32	1.05	b.d.l.	129100	85.7	1.40	7.50	451440	n.d.
	27.7.01	50.1	12.9	0.21	1.33	5.1	133900	85.9	n.d.	7.55	n.d.	n.d.
	31.7.01	55.1	14.4	0.59	1.31	2.8	129990	86.1	n.d.	7.54	n.d.	n.d.
	3.8.01	55.8	8.8	0.16	1.35	b.d.l.	129400	84.9	1.18	7.61	n.d.	n.d.
	7.8.01	56.5	7.5	b.d.l.	1.06	b.d.l.	124500	88.9	1.35	7.05	n.d.	n.d.
	10.8.01	66.6	14.7	0.10	1.23	1.4	128300	86.3	1.38	7.15	n.d.	n.d.
	13.8.01	83.3	21.0	0.20	1.50	7.5	139000	86.1	1.44	7.10	n.d.	n.d.
	16.8.01	86.3	20.2	0.25	1.69	3.9	136000	86.4	1.44	7.11	n.d.	n.d.
	24.8.01	85.6	3.6	0.31	1.56	b.d.l.	137000	86.1	1.20	7.11	n.d.	n.d.
	31.8.01	67.0	11.9	0.16	0.96	b.d.l.	133800	86.1	1.18	7.13	577000	n.d.
	7.9.01	61.3	2.0	b.d.l.	0.60	b.d.l.	127600	87.4	0.90	7.15	515400	n.d.
14.9.01	100.7	2.0	0.11	0.65	b.d.l.	125000	88.1	1.17	7.08	n.d.	n.d.	
18.9.01	65.9	2.0	0.05	0.53	b.d.l.	124100	86.5	1.09	7.03	446000	n.d.	
25.9.01	57.4	5.7	0.09	0.37	3.1	124000	88.7	1.17	7.20	n.d.	n.d.	

Table. 1. Continued.

samples	date	He	H ₂	O ₂	N ₂	CO	CH ₄	CO ₂	$\delta^{13}\text{C}_{\text{CO}_2}$	He R/Ra	CO ₂ dyn	T°C
P39	2.10.01	98.5	9.2	0.04	0.18	b.d.l.	129900	87.6	1.11	7.21	n.d.	n.d.
	9.10.01	58.1	9.2	0.04	0.91	b.d.l.	132700	87.0	1.13	7.17	599976	n.d.
	16.10.01	n.d.	n.d.	n.d.	n.d.	n.d.	n.d.	n.d.	0.96	6.95	n.d.	n.d.
	23.10.01	73.2	5.1	0.16	1.04	2.6	126900	87.0	1.07	7.13	n.d.	n.d.
	29.10.01	90.8	6.3	0.05	0.72	1.9	125500	86.8	1.23	7.29	n.d.	n.d.
	7.11.01	69.7	7.2	0.07	0.78	11.7	128700	86.3	n.d.	n.d.	n.d.	n.d.
	13.11.01	83.8	b.d.l.	0.11	0.69	b.d.l.	124000	87.7	1.11	7.34	n.d.	n.d.
	22.11.01	84.7	b.d.l.	0.32	0.94	b.d.l.	133600	85.0	1.06	7.37	630800	n.d.
	27.11.01	58.2	b.d.l.	b.d.l.	0.70	5.2	129100	87.4	0.99	7.32	n.d.	n.d.
	5.12.01	64.4	4.3	0.11	0.74	5.2	127600	87.8	0.97	7.34	n.d.	n.d.
	11.12.01	73.3	b.d.l.	0.00	0.68	10.4	132000	87.0	0.92	7.25	n.d.	n.d.
	20.12.01	90.0	b.d.l.	0.14	0.94	5.1	135900	86.7	0.77	n.d.	730700	n.d.
	28.12.01	86.3	b.d.l.	0.12	0.84	b.d.l.	128700	86.0	0.94	n.d.	n.d.	n.d.
	9.1.02	67.6	b.d.l.	b.d.l.	0.57	b.d.l.	126900	88.00	0.88	7.35	n.d.	n.d.
	9.1.02	74.7	b.d.l.	0.21	1.08	b.d.l.	126000	86.10	0.88	n.d.	n.d.	n.d.
	22.1.02	93.4	b.d.l.	0.05	0.86	7.8	128500	86.95	0.97	n.d.	n.d.	n.d.
	23.1.02	61.4	11.5	0.05	0.61	b.d.l.	123200	88.01	1.08	n.d.	750000	n.d.
	5.2.02	95.7	b.d.l.	0.24	0.71	b.d.l.	124800	86.44	1.17	7.40	900000	n.d.
	7.2.02	87.6	b.d.l.	0.07	0.62	b.d.l.	120500	87.59	1.07	7.37	n.d.	n.d.
	14.2.02	n.d.	n.d.	n.d.	n.d.	n.d.	n.d.	n.d.	1.22	n.d.	n.d.	n.d.
	20.2.02	76.8	b.d.l.	0.16	0.90	b.d.l.	121500	87.41	1.17	n.d.	900000	n.d.
	4.3.02	66.2	b.d.l.	0.74	2.38	b.d.l.	116600	85.29	1.15	n.d.	807660	n.d.
	12.3.02	71.6	b.d.l.	b.d.l.	0.68	b.d.l.	128300	86.61	1.17	7.25	n.d.	n.d.
	19.3.02	68.1	b.d.l.	n.d.	0.60	3.7	123100	86.81	1.16	n.d.	438444	n.d.
	26.3.02	77.2	b.d.l.	n.d.	0.02	b.d.l.	123900	89.35	1.07	7.01	423060	n.d.
	4.4.02	75.8	b.d.l.	n.d.	0.53	b.d.l.	122600	88.70	1.10	n.d.	n.d.	n.d.
	9.4.02	71.5	b.d.l.	n.d.	0.63	b.d.l.	121500	87.90	1.29	7.00	n.d.	n.d.
	18.4.02	67.2	b.d.l.	b.d.l.	0.46	b.d.l.	111000	88.42	1.13	n.d.	n.d.	n.d.
	23.4.02	n.d.	n.d.	n.d.	n.d.	n.d.	n.d.	n.d.	1.24	6.97	n.d.	n.d.
	3.5.02	68.2	b.d.l.	0.44	1.68	b.d.l.	120400	85.92	1.23	n.d.	403830	n.d.
	7.5.02	73.5	b.d.l.	0.00	0.39	b.d.l.	124500	87.58	1.24	6.91	n.d.	n.d.
	16.5.02	61.9	b.d.l.	0.47	1.99	b.d.l.	132700	84.40	1.45	n.d.	442290	n.d.
	21.5.02	75.0	b.d.l.	0.00	0.62	b.d.l.	118700	87.56	1.33	6.89	n.d.	n.d.
	30.5.02	74.4	b.d.l.	0.30	0.80	b.d.l.	124500	86.86	1.29	n.d.	n.d.	n.d.
	4.6.02	82.5	b.d.l.	0.00	0.56	b.d.l.	122800	87.20	1.24	6.94	n.d.	n.d.
	17.6.02	59.0	b.d.l.	0.29	0.78	b.d.l.	118800	87.28	1.48	6.90	n.d.	n.d.
	24.6.02	67.8	b.d.l.	0.77	3.19	3.3	113600	85.06	1.39	n.d.	307700	n.d.
	1.7.02	89.8	9.8	0.27	0.65	b.d.l.	120500	87.17	1.28	6.90	n.d.	n.d.
	16.7.02	68.7	7.5	0.23	0.74	b.d.l.	119100	87.29	1.37	6.83	238450	n.d.
	23.7.02	60.8	b.d.l.	1.34	6.69	b.d.l.	108200	81.22	1.24	n.d.	n.d.	n.d.
	31.7.02	78.3	b.d.l.	b.d.l.	0.79	b.d.l.	121800	87.14	1.16	6.70	n.d.	n.d.
	13.8.02	90.9	15.3	0.30	1.10	1.1	122900	86.41	1.33	6.65	n.d.	n.d.
	28.8.02	67.4	7.9	b.d.l.	1.29	b.d.l.	122300	86.54	1.26	6.73	n.d.	n.d.
	12.9.02	73.5	6.7	b.d.l.	1.03	b.d.l.	124600	86.77	n.d.	6.83	n.d.	n.d.
	16.9.02	58.9	b.d.l.	2.64	14.14	2.9	100300	73.40	1.59	n.d.	246144	n.d.
	24.9.02	85.1	b.d.l.	0.15	1.28	b.d.l.	123000	86.73	1.29	6.91	n.d.	n.d.
	10.10.02	77.6	b.d.l.	b.d.l.	0.72	b.d.l.	123700	86.97	1.07	6.99	n.d.	n.d.
	12.10.02	73.5	6.6	0.00	1.03	b.d.l.	124600	86.77	1.04	n.d.	269200	n.d.
	21.10.02	85.9	b.d.l.	0.09	0.78	b.d.l.	122800	86.99	1.12	7.17	n.d.	n.d.
	27.10.02	105.0	b.d.l.	0.30	1.13	b.d.l.	131400	85.80	1.00	7.02	n.d.	n.d.
	31.10.02	75.7	b.d.l.	0.12	0.77	1.3	125200	86.61	1.12	6.91	292300	n.d.
	4.11.02	81.9	b.d.l.	0.10	0.82	b.d.l.	125100	86.67	1.04	6.86	n.d.	n.d.

Table. 1. Continued.

samples	date	He	H ₂	O ₂	N ₂	CO	CH ₄	CO ₂	$\delta^{13}\text{C}_{\text{CO}_2}$	He R/Ra	CO ₂ dyn	T°C
P39	8.11.02	67.8	b.d.l.	b.d.l.	0.65	b.d.l.	128200	86.75	1.01	6.93	392300	n.d.
	11.11.02	92.5	b.d.l.	0.32	1.01	b.d.l.	132800	85.47	1.06	6.94	n.d.	n.d.
	14.11.02	62.8	b.d.l.	0.00	0.51	b.d.l.	122800	87.29	0.98	6.90	569200	n.d.
	18.11.02	74.5	b.d.l.	0.04	0.56	b.d.l.	123800	87.16	1.08	6.89	n.d.	n.d.
	21.11.02	73.2	b.d.l.	0.20	0.79	b.d.l.	127600	86.88	1.04	6.97	407700	n.d.
	25.11.02	76.7	b.d.l.	0.97	6.60	b.d.l.	122800	80.54	1.06	7.00	900000	n.d.
	2.12.02	70.6	b.d.l.	0.08	0.61	b.d.l.	124300	87.19	1.11	6.33	n.d.	n.d.
	4.12.02	n.d.	n.d.	n.d.	n.d.	n.d.	n.d.	n.d.	n.d.	n.d.	800000	n.d.
	8.12.02	n.d.	n.d.	n.d.	n.d.	n.d.	n.d.	n.d.	1.13	6.50	n.d.	n.d.
	11.12.02	79.4	b.d.l.	b.d.l.	0.60	b.d.l.	129500	86.65	1.06	6.45	630744	n.d.
	17.12.02	70.1	b.d.l.	b.d.l.	0.60	b.d.l.	119800	87.55	n.d.	6.49	553800	n.d.
	24.12.02	74.5	b.d.l.	b.d.l.	0.52	b.d.l.	121700	87.76	n.d.	6.46	n.d.	n.d.
	27.12.02	72.1	b.d.l.	b.d.l.	0.50	b.d.l.	133800	87.28	n.d.	n.d.	n.d.	n.d.
	8.1.03	73.6	b.d.l.	0.03	0.51	b.d.l.	123400	87.39	n.d.	n.d.	n.d.	n.d.
	14.1.03	n.d.	n.d.	n.d.	n.d.	n.d.	n.d.	n.d.	n.d.	n.d.	557670	n.d.
	16.1.03	70.1	b.d.l.	b.d.l.	0.60	b.d.l.	119800	87.55	1.04	6.44	n.d.	n.d.
	20.1.03	n.d.	n.d.	n.d.	n.d.	n.d.	n.d.	n.d.	1.08	n.d.	n.d.	n.d.
	23.1.03	58.5	b.d.l.	b.d.l.	0.51	b.d.l.	121300	88.10	1.09	6.44	n.d.	n.d.
	30.1.03	72.4	b.d.l.	0.04	0.54	b.d.l.	123000	87.44	1.20	6.45	869200	n.d.
	5.2.03	75.4	b.d.l.	b.d.l.	0.51	b.d.l.	123900	87.64	1.12	6.38	n.d.	n.d.
	19.2.03	64.8	b.d.l.	0.10	0.73	b.d.l.	121000	87.25	1.09	n.d.	953800	n.d.
	22.2.03	66.1	b.d.l.	b.d.l.	0.47	b.d.l.	125300	87.19	1.11	6.34	n.d.	n.d.
	12.3.03	74.4	b.d.l.	0.06	0.56	b.d.l.	126300	87.59	n.d.	6.27	n.d.	n.d.
	13.3.03	67.1	b.d.l.	0.14	0.67	b.d.l.	124200	86.82	1.14	n.d.	800000	n.d.
	2.4.03	52.6	b.d.l.	0.03	0.46	b.d.l.	130200	87.07	1.08	6.46	n.d.	n.d.
	14.4.03	63.7	b.d.l.	b.d.l.	0.51	b.d.l.	130400	86.55	1.23	n.d.	n.d.	n.d.
	16.4.03	60.0	b.d.l.	b.d.l.	0.65	b.d.l.	134300	46.36	1.33	6.43	769200	n.d.
	6.5.03	49.6	b.d.l.	b.d.l.	0.69	b.d.l.	127600	86.65	1.43	6.49	n.d.	n.d.
	9.5.03	56.8	b.d.l.	b.d.l.	1.19	21.5	122100	87.03	1.31	n.d.	792300	n.d.
	30.5.03	57.3	b.d.l.	b.d.l.	0.59	b.d.l.	134500	86.16	1.20	6.21	n.d.	n.d.
	13.6.03	n.d.	n.d.	n.d.	n.d.	n.d.	n.d.	n.d.	1.35	6.27	n.d.	n.d.
	17.6.03	47.9	b.d.l.	0.52	4.69	2.6	113700	84.06	1.17	n.d.	515370	n.d.
	24.6.03	n.d.	n.d.	n.d.	n.d.	n.d.	n.d.	n.d.	1.32	6.39	392300	n.d.
17.7.03	55.8	b.d.l.	b.d.l.	0.64	1.0	110900	88.68	1.35	n.d.	500000	n.d.	
VS	6.7.00	142.2	b.d.l.	0.62	2.4	b.d.l.	369000	63.1	-2.66	6.84	n.d.	n.d.
	3.8.00	110.8	b.d.l.	0.10	0.8	b.d.l.	339300	62.7	-3.04	6.43	n.d.	n.d.
	30.8.00	99.7	4.4	0.07	0.7	b.d.l.	318000	72.4	-2.97	6.59	n.d.	n.d.
	15.9.00	153.2	b.d.l.	1.16	5.3	b.d.l.	448000	53.7	-2.83	6.42	n.d.	n.d.
	3.10.00	142.0	b.d.l.	0.27	1.3	b.d.l.	443000	54.8	-2.83	6.84	n.d.	n.d.
	18.10.00	107.0	b.d.l.	0.07	0.3	b.d.l.	215000	78.5	-3.52	6.78	n.d.	n.d.
	9.11.00	110.6	b.d.l.	0.49	2.2	b.d.l.	289000	68.7	-3.39	6.78	n.d.	n.d.
	30.11.00	n.d.	n.d.	n.d.	n.d.	n.d.	n.d.	n.d.	-2.10	n.d.	n.d.	n.d.
	6.12.00	139.0	b.d.l.	0.03	0.7	b.d.l.	334000	68.2	-3.28	6.65	n.d.	n.d.
	19.12.00	153.5	b.d.l.	2.02	7.5	b.d.l.	373000	53.8	-3.15	6.65	n.d.	n.d.
	11.1.01	115.3	b.d.l.	0.10	0.7	b.d.l.	349500	66.5	-3.31	6.74	n.d.	n.d.
	22.1.01	238.0	b.d.l.	0.12	1.0	b.d.l.	555000	45.4	-2.03	6.58	n.d.	n.d.
	10.2.01	182.4	b.d.l.	0.02	0.2	b.d.l.	533000	47.9	-2.51	6.87	n.d.	n.d.
	27.2.01	109.0	b.d.l.	0.07	0.6	b.d.l.	383500	64.9	-3.40	6.63	n.d.	n.d.
	22.3.01	181.8	b.d.l.	b.d.l.	0.5	b.d.l.	432000	60.2	-3.02	6.49	n.d.	n.d.

Table. 1. Continued.

samples	date	He	H ₂	O ₂	N ₂	CO	CH ₄	CO ₂	$\delta^{13}\text{C}_{\text{CO}_2}$	He R/Ra	CO ₂ dyn	T°C
VS	11.4.01	166.2	b.d.l.	1.53	5.3	b.d.l.	434000	51.4	-1.43	6.52	n.d.	n.d.
	2.5.01	116.0	b.d.l.	0.07	0.5	b.d.l.	332000	67.6	-2.30	6.57	n.d.	n.d.
	16.5.01	249.0	b.d.l.	0.06	0.8	b.d.l.	509100	50.9	-2.40	6.66	n.d.	n.d.
	5.6.01	172.0	b.d.l.	b.d.l.	0.6	2.8	427000	58.7	-2.96	6.57	n.d.	n.d.
	28.6.01	204.1	b.d.l.	0.13	0.8	2.3	383300	63.7	-2.51	6.69	n.d.	n.d.
	12.7.01	208.3	b.d.l.	b.d.l.	0.7	b.d.l.	397400	52.8	-2.32	6.87	n.d.	n.d.
	17.7.01	204.8	b.d.l.	0.15	0.7	b.d.l.	458600	59.8	-2.83	6.90	n.d.	n.d.
	24.7.01	281.0	b.d.l.	b.d.l.	1.0	b.d.l.	490200	50.0	-2.15	7.06	n.d.	n.d.
	27.7.01	169.0	b.d.l.	b.d.l.	0.7	b.d.l.	441800	56.0	n.d.	7.12	n.d.	n.d.
	3.8.01	120.0	b.d.l.	b.d.l.	0.5	b.d.l.	309000	70.1	-3.17	7.08	n.d.	n.d.
	7.8.01	280.4	b.d.l.	b.d.l.	1.0	b.d.l.	560400	45.0	n.d.	6.76	n.d.	n.d.
	10.8.01	229.5	b.d.l.	1.17	5.3	b.d.l.	458000	49.0	-2.27	6.87	n.d.	n.d.
	13.8.01	151.1	b.d.l.	b.d.l.	0.8	b.d.l.	351000	65.6	-3.19	6.72	n.d.	n.d.
	16.8.01	156.0	b.d.l.	1.73	8.1	1.9	381400	55.0	-2.83	6.71	n.d.	n.d.
	24.8.01	n.d.	n.d.	n.d.	n.d.	n.d.	n.d.	n.d.	-3.15	6.68	n.d.	n.d.
	30.8.01	117.4	b.d.l.	b.d.l.	0.5	3.4	266300	73.7	-3.80	6.66	n.d.	n.d.
	7.9.01	203.0	b.d.l.	0.07	0.6	b.d.l.	336000	66.2	-3.28	6.65	n.d.	n.d.
	14.9.01	139.4	b.d.l.	b.d.l.	0.5	b.d.l.	358000	67.6	-3.60	6.64	n.d.	n.d.
	18.9.01	279.8	b.d.l.	0.80	2.1	b.d.l.	510000	53.5	-2.24	6.57	n.d.	n.d.
	25.9.01	107.0	b.d.l.	0.01	0.2	b.d.l.	271400	73.9	-3.42	6.68	n.d.	n.d.
	2.10.01	122.4	b.d.l.	0.02	0.2	b.d.l.	297000	71.4	-3.33	6.71	n.d.	n.d.
	9.10.01	137.0	b.d.l.	0.01	0.7	b.d.l.	371200	64.0	-3.17	6.70	n.d.	n.d.
	16.10.01	n.d.	n.d.	n.d.	n.d.	n.d.	n.d.	n.d.	-2.79	6.49	n.d.	n.d.
	23.10.01	n.d.	n.d.	n.d.	n.d.	n.d.	n.d.	n.d.	-3.17	6.66	n.d.	n.d.
	7.11.01	136.5	7.5	0.50	0.5	22.2	315400	67.6	-2.95	7.06	n.d.	n.d.
	13.11.01	190.6	b.d.l.	0.06	1.0	2.2	342400	65.7	-2.73	6.77	n.d.	n.d.
	21.11.01	134.0	b.d.l.	0.06	0.8	b.d.l.	331000	67.0	-2.76	6.90	n.d.	n.d.
	23.11.01	n.d.	n.d.	n.d.	n.d.	n.d.	n.d.	n.d.	-3.33	n.d.	n.d.	n.d.
	27.11.01	126.0	b.d.l.	0.09	0.6	b.d.l.	347700	66.0	-3.09	6.82	n.d.	n.d.
	6.12.01	154.0	b.d.l.	0.16	1.1	b.d.l.	337600	65.7	-2.98	6.87	n.d.	n.d.
	11.12.01	172.4	b.d.l.	b.d.l.	0.5	b.d.l.	360100	64.2	-3.20	6.75	n.d.	n.d.
	18.12.01	n.d.	n.d.	n.d.	n.d.	n.d.	n.d.	n.d.	-3.22	n.d.	n.d.	n.d.
	20.12.01	182.2	b.d.l.	0.37	1.5	b.d.l.	352600	63.5	n.d.	n.d.	n.d.	n.d.
	28.12.01	207.5	b.d.l.	b.d.l.	0.9	b.d.l.	461800	53.5	-0.63	n.d.	n.d.	n.d.
	9.1.02	170.4	b.d.l.	b.d.l.	0.5	b.d.l.	338400	67.0	-3.21	6.67	n.d.	n.d.
	10.1.02	171.4	b.d.l.	0.54	0.6	b.d.l.	324100	67.6	n.d.	6.81	n.d.	n.d.
	22.1.02	n.d.	n.d.	n.d.	n.d.	n.d.	n.d.	n.d.	-3.82	n.d.	n.d.	n.d.
	23.1.02	139.7	b.d.l.	0.12	0.8	b.d.l.	324800	67.1	-1.08	n.d.	n.d.	n.d.
	4.2.02	154.3	b.d.l.	1.43	3.4	b.d.l.	354700	60.3	-3.24	6.69	n.d.	n.d.
	6.2.02	105.5	10.2	9.40	36.7	12.4	237900	30.9	-3.29	n.d.	n.d.	n.d.
	7.2.02	175.2	b.d.l.	0.13	0.9	b.d.l.	331600	66.7	-3.13	6.70	n.d.	n.d.
	20.2.02	169.6	b.d.l.	0.62	2.2	b.d.l.	334200	64.5	-3.06	6.67	n.d.	n.d.
	4.3.02	154.3	b.d.l.	1.43	3.4	b.d.l.	354700	60.3	-2.36	n.d.	n.d.	n.d.
	12.3.02	243.4	b.d.l.	b.d.l.	1.1	b.d.l.	430800	55.8	-1.95	6.47	n.d.	n.d.
	19.3.02	167.0	b.d.l.	0.50	2.2	b.d.l.	355800	68.9	-2.99	n.d.	n.d.	n.d.
	26.3.02	196.1	b.d.l.	b.d.l.	0.5	b.d.l.	424000	59.1	-2.52	6.58	n.d.	n.d.
	5.4.02	253.0	b.d.l.	b.d.l.	1.0	b.d.l.	424500	57.1	-2.13	n.d.	n.d.	n.d.
	9.4.02	n.d.	n.d.	n.d.	n.d.	n.d.	n.d.	n.d.	-3.70	6.48	n.d.	n.d.
	17.4.02	227.3	b.d.l.	0.28	1.0	b.d.l.	434200	56.1	-2.84	n.d.	n.d.	n.d.
	23.4.02	n.d.	n.d.	n.d.	n.d.	n.d.	n.d.	n.d.	-3.24	6.41	n.d.	n.d.
	3.5.02	239.6	b.d.l.	b.d.l.	0.7	b.d.l.	465700	53.2	-2.00	n.d.	n.d.	n.d.
	15.5.02	154.7	b.d.l.	b.d.l.	0.5	b.d.l.	341600	65.7	-3.20	6.32	n.d.	n.d.

Table 1. Continued.

samples	date	He	H ₂	O ₂	N ₂	CO	CH ₄	CO ₂	$\delta^{13}\text{C}_{\text{cor}}$	He R/Ra	CO ₂ dyn	T°C
VS	16.5.02	75.3	b.d.l.	0.82	3.2	b.d.l.	211600	75.0	-3.03	n.d.	n.d.	n.d.
	21.5.02	48.5	b.d.l.	14.10	55.4	13.5	96000	20.9	-2.95	n.d.	n.d.	n.d.
	30.5.02	183.0	b.d.l.	0.42	1.6	b.d.l.	349000	63.3	-2.56	n.d.	n.d.	n.d.
	4.6.02	156.1	40.1	b.d.l.	0.6	b.d.l.	324300	67.1	-2.79	6.32	n.d.	n.d.
	17.6.02	158.8	b.d.l.	0.27	1.0	b.d.l.	325900	66.2	-2.33	6.35	n.d.	n.d.
	24.6.02	146.2	b.d.l.	0.65	2.3	b.d.l.	340600	63.1	-2.83	n.d.	n.d.	n.d.
	1.7.02	293.6	b.d.l.	0.98	4.5	b.d.l.	457400	49.6	-3.49	6.32	n.d.	n.d.
	16.7.02	166.6	b.d.l.	b.d.l.	0.6	b.d.l.	329700	66.5	-2.88	6.34	n.d.	n.d.
	23.7.02	260.0	b.d.l.	0.58	1.8	b.d.l.	477400	50.1	-1.72	n.d.	n.d.	n.d.
	31.7.02	172.3	b.d.l.	b.d.l.	0.7	4.7	310700	68.6	-2.70	6.31	n.d.	n.d.
	13.8.02	215.0	b.d.l.	b.d.l.	1.0	b.d.l.	351600	64.1	n.d.	6.31	n.d.	n.d.
	28.8.02	254.1	12.8	b.d.l.	1.1	b.d.l.	482700	50.8	-2.44	6.37	n.d.	n.d.
	10.9.02	176.3	b.d.l.	b.d.l.	1.0	b.d.l.	328100	66.3	n.d.	6.40	n.d.	n.d.
	16.9.02	233.5	b.d.l.	0.47	1.2	b.d.l.	436700	54.7	-2.25	n.d.	n.d.	n.d.
	24.9.02	243.3	b.d.l.	1.58	6.4	1.4	383000	54.2	-2.08	6.53	n.d.	n.d.
	10.10.02	210.4	b.d.l.	0.03	0.7	b.d.l.	422100	57.1	-2.31	6.58	n.d.	n.d.
	22.10.02	314.3	b.d.l.	b.d.l.	1.3	b.d.l.	502700	48.9	-1.74	6.54	n.d.	n.d.
	27.10.02	333.0	b.d.l.	0.18	1.7	b.d.l.	501300	47.2	-1.51	6.53	n.d.	n.d.
	30.10.02	270.8	b.d.l.	1.18	4.9	2.0	467400	49.3	-1.74	6.52	n.d.	n.d.
	4.11.02	321.8	b.d.l.	b.d.l.	0.9	b.d.l.	502800	49.0	-2.21	6.51	n.d.	n.d.
	8.11.02	312.7	b.d.l.	b.d.l.	1.5	b.d.l.	517100	47.3	-2.00	6.46	n.d.	n.d.
	11.11.02	301.7	b.d.l.	0.08	1.2	b.d.l.	479700	50.8	-1.95	6.45	n.d.	n.d.
	14.11.02	259.7	b.d.l.	0.00	0.8	2.0	440800	55.7	-2.18	6.41	n.d.	n.d.
	19.11.02	244.9	b.d.l.	0.64	2.4	2.0	432500	53.7	-3.13	6.35	n.d.	n.d.
	21.11.02	203.6	b.d.l.	0.11	1.4	b.d.l.	433800	55.2	-2.23	6.49	n.d.	n.d.
	25.11.02	n.d.	n.d.	n.d.	n.d.	n.d.	n.d.	n.d.	-2.97	n.d.	n.d.	n.d.
	2.12.02	264.1	b.d.l.	b.d.l.	1.0	b.d.l.	486100	50.7	-1.79	6.41	n.d.	n.d.
	11.12.02	271.3	b.d.l.	b.d.l.	0.9	b.d.l.	450800	54.1	-2.15	6.57	n.d.	n.d.
	17.12.02	271.0	b.d.l.	b.d.l.	1.4	b.d.l.	474900	51.2	-2.16	6.56	n.d.	n.d.
	24.12.02	193.9	b.d.l.	b.d.l.	0.9	b.d.l.	454800	53.7	-1.96	6.45	n.d.	n.d.
	27.12.02	169.6	b.d.l.	1.15	5.4	b.d.l.	381200	55.6	-2.24	6.47	n.d.	n.d.
	8.1.03	134.4	b.d.l.	2.57	10.0	b.d.l.	284800	59.2	-3.04	6.34	n.d.	n.d.
	16.1.03	203.5	b.d.l.	b.d.l.	0.9	b.d.l.	441400	55.8	-2.05	6.36	n.d.	n.d.
	23.1.03	169.4	b.d.l.	0.03	0.9	b.d.l.	384000	61.2	-2.29	6.28	n.d.	n.d.
	30.1.03	151.2	b.d.l.	b.d.l.	0.7	2.5	407700	58.8	-2.28	6.33	n.d.	n.d.
	6.2.03	202.2	b.d.l.	b.d.l.	1.0	b.d.l.	460000	53.3	-2.03	6.41	n.d.	n.d.
	22.2.03	n.d.	n.d.	n.d.	n.d.	n.d.	n.d.	n.d.	-3.61	6.36	n.d.	n.d.
	12.3.03	148.2	b.d.l.	5.50	22.3	1.7	304600	42.1	-2.36	6.48	n.d.	n.d.
	2.4.03	167.3	b.d.l.	b.d.l.	0.6	b.d.l.	406000	58.8	-2.24	6.57	n.d.	n.d.
	14.4.03	176.4	b.d.l.	1.01	4.4	b.d.l.	439700	50.7	-2.34	6.51	n.d.	n.d.
	6.5.03	150.9	b.d.l.	2.19	10.7	2.9	412100	45.9	-2.25	6.49	n.d.	n.d.
	9.5.03	221.1	b.d.l.	b.d.l.	0.7	b.d.l.	470700	52.6	-2.36	n.d.	n.d.	n.d.
	30.5.03	72.5	b.d.l.	b.d.l.	0.3	b.d.l.	281600	73.0	-2.06	6.29	n.d.	n.d.
	13.6.03	n.d.	n.d.	n.d.	n.d.	n.d.	n.d.	n.d.	-3.36	6.44	n.d.	n.d.
	17.6.03	175.3	b.d.l.	b.d.l.	1.3	5.0	485500	51.0	-1.97	n.d.	n.d.	n.d.
	24.6.03	n.d.	n.d.	n.d.	n.d.	n.d.	n.d.	n.d.	-2.11	6.62	n.d.	n.d.
	3.7.03	78.3	b.d.l.	b.d.l.	0.2	b.d.l.	274400	72.9	-3.676	6.42	n.d.	n.d.
	17.7.03	283.0	2.0	b.d.l.	1.0	b.d.l.	539300	45.9	-1.39	n.d.	n.d.	n.d.

3. ETNA PLUMBING SYSTEM

3.1 Deep Magma Reservoir

Several lines of evidence indicate that Mt. Etna's plumbing system is quite complex. Geophysical, petrological and geochemical evidences strongly support the existence of a large and deep magma reservoir beneath Mt. Etna. These include the distribution of hypocentral depths of volcanic earthquakes (Cardaci et al. 1993), the detection of an upwarped lower-crust boundary beneath the volcano from seismic refraction studies (Hirn et al. 1997), large-scale ground deformation of the volcanic pile associated with recent large eruptions (Bonaccorso et al. 1994; Bonaccorso 1996), ^{226}Re - ^{230}Th radioactive disequilibria studies (Condomines et al. 1995), and overall chemical composition of recently erupted lavas (Tanguy et al. 1997). The width of this reservoir was estimated by Sharp et al. (1980) to be in the range of 20 to 30 km. More recently, Caracausi et al. (2003a) indicated a minimum width of 60 km for this reservoir. The depth of this reservoir was estimated at about 20 km below sea level (Hirn et al. 1997) and its nature was identified by Allard (1997), D'Alessandro et al. (1997b) and Caracausi et al. (2003a) as an up-warped asthenosphere where large convective movements of molten material take place. This assumption was based on the large imbalance between volumes of erupted lava and volumes of non-eruptive degassing magma inferred from the budget of volcanic gas emitted from Mt. Etna (the latter is about 10 times higher than the former). Gvirtzman and Nur (1999) related the asthenospheric upwelling underneath Mt. Etna to slab rollback in the south Tyrrhenian subduction zone.

3.2 Shallow Magma Reservoirs

Shallow magma reservoirs were also identified beneath Mt. Etna mainly on the basis of ground deformation (Bonaccorso et al. 1994; Bonaccorso 1996) and seismic data (Murru et al. 1999; Patanè et al. 2003). In particular, Murru et al. (1999) found evidence of at least two magma reservoirs. One has a radius less than 2 km and is located WSW of the summit at about 3 ± 2 km b.s.l.; the other has a radius less than 5 km and is located 2 km E of the summit at about 10 ± 3 km b.s.l.. According to Murray (1990), such shallow reservoirs are temporary and are occupied by magma only during the relatively short periods (a few days to a few years) that precede eruptions. However, it cannot be excluded that some degassed magma can occupy those shallow reservoirs for longer times and is periodically replaced by fresh, gas-rich magma, hence producing small-scale convective overturn of magma within the upper feeding system of the volcano, as already suggested by Allard (1997) and Bruno et al. (1999). According to these authors, degassed magma would tend to sink down into the magma column due to its increased density and would be in part recycled and in part stored into intrusive bodies at depth within the crust.

4. VOLCANIC ACTIVITY DURING THE PERIOD JULY 2000 - JULY 2003

During the period of the present study volcanic activity at Mt. Etna was remarkable, par-

ticularly at the South-east crater (henceforth indicated with SEC), varying from strong strombolian explosions to violent lava fountaining to eventually a lateral eruption.

The first eruptive episodes occurred at the SEC on August 28 and 29, 2000. Both were paroxysmal episodes, consisting of violent lava fountaining from the SEC's main vent or from secondary vents that opened along fissures at the crater's foot. This explosive activity was accompanied by emission of fluid lava flows. At the end of November the SEC re-activated with about ten days of weak summit strombolian activity. Then, for about two weeks a slow and viscous lava flow was gently emitted from its northeastern slope and produced a small lava flow field. Afterwards, eruptive activity resumed at SEC on January 20, 2001. Lava was discontinuously effused until July 2001, often accompanied by strombolian explosions or lava fountaining, with an output rate ranging from 1 to 10 m³ s⁻¹. In particular, a new short cycle of strong paroxysmal events started on June 7, 2001. The intensity of such episodes was ever increasing with emission of well-fed lava flows from the NE foot of the cone. Simultaneously, strong strombolian activity, often evolving to short-lived lava fountaining, took place at the top of the cone. This cycle ended on July 17 after 15 eruptive episodes, followed right after by the complex sub-terminal and lateral July-August 2001 eruption.

During the period preceding the July-August 2001 eruption, a progressive increase in strombolian activity at the Bocca Nuova was observed. Periodic explosions occurred mainly during the period September-October 2000 and more evidently in February-March 2001, when bursts of lava increased both in frequency and intensity. At the end of February 2001 weak explosive activity resumed at North-East Crater, too. Conversely, the Voragine showed only quiet degassing activity throughout the whole period.

After a strong seismic swarm on July 12, between July 13 and July 20 a 7 km-long system of dry fractures formed on the upper southern flank of Mt. Etna, starting from the southern side of the SEC at about 2900 m a.s.l., mainly oriented N-S. This fissure developed further south down to 2700 m of altitude. A few days later, another fissure formed on the uppermost NE flank of the volcano, again starting from the SEC. Lava was erupted from several points along the two fissures. The main lava flows were emitted from the lower southern fissure, and flowed down to an altitude of 1040 m a.s.l.. The eruption ended on August 9, 2001, after emitting a volume of lava estimated between 30 (Behncke and Neri 2003) and 48 million m³ (INGV-CT 2001).

The 2001 eruption was followed by periodic ash emission and weak to strong strombolian activity at North-east crater and Bocca Nuova. Between the 26 and the 27 of October 2002 a new flank eruption started both along the North-east Rift (where the eruptive activity stopped on November 5) and on the upper southern flank of the volcano. Here the eruption was more intense and lasted for three months. It formed two large cones at about 2750 - 2800 m a.s.l. and a highly composed lava flow field. A 2 - 3 km-high sustained eruptive column produced an abundant ash and tephra fallout for most of the first two months of eruption, then the explosive and effusive activity gradually decreased and on January 28, 2003 the eruption ended.

5. CHEMICAL CHARACTERIZATION OF ETNA'S SOIL AND FUMAROLE GASES

Carbon dioxide is the major constituent of gas samples from the low altitude sites (Naftia, VS and P39), followed by CH₄ and He, CO and H₂. Conversely, all other samples show remarkable air pollution, as evidenced by the high amounts of O₂ and N₂, followed by CO₂ and by variable concentrations of CO, CH₄, H₂ and He. This feature is due to the combined effect of high soil permeability and relatively low, although anomalous, gas flux through the ground. Among the air-contaminated sites, that of BLV deserves a particular attention, because the fumaroles there present are characterised by the highest temperature (84.8 to 105.0°C), the highest concentration of CO₂ and He values slightly exceeding that of air (5.4 ppmv).

According to Giammanco et al. (1998a, and literature therein cited), the high concentrations of CH₄ and He in the gas samples from sites P39, VS and Naftia (Fig. 2) would result from CO₂ depletion in the gas phase after interaction between deep CO₂-rich gases and shallow CO₂ unsaturated groundwaters. This phenomenon causes He enrichment in the residual gas phase and its intensity is a function of both the pH of water and the flux of incoming CO₂ that interacts with the aquifer. Methane enrichment relative to CO₂ is particularly evident in the samples from site P39 and even more so in those from VS (Fig. 2). This can be in part explained by interactions between magmatic gas and CO₂-unsaturated groundwater similar to those inferred for the He enrichment, because CH₄ has a solubility coefficient (18 ml l⁻¹) much lower than that of CO₂ (759 ml l⁻¹) and close to that of He (8.75 ml l⁻¹) (Capasso and Inguaggiato 1998). In addition to this, interactions between magmatic gas and relatively shallow hydrocarbon reservoirs can also be invoked, as deduced by Parello et al. (1995) and Giammanco et al. (1998a) and confirmed by the isotopic composition of carbon and deuterium of CH₄ (Grassa et al. 2004).

6. He AND C_(CO₂) ISOTOPES OF ETNA'S GASES

6.1 Isotopic Markers of C and He of Etna's Magma

In recent years, many studies were aimed at assessing the pristine isotopic composition of helium and carbon of CO₂ in Etna's magma. The reason for this lies in the differences between Etna's values and those typical of MORBs. According to the classic interpretations (e.g., Taylor et al. 1967; Deines 1970; Allard 1983, 1986), MORB values of $\delta^{13}\text{C}_{(\text{CO}_2)}$ range from -8 to -5‰ and those of He are 8 ± 1 Ra. R/Ra values in inferred Etna's magmatic end-member (< 8 Ra) are always lower than MORB ones. Inferred magmatic values of $\delta^{13}\text{C}_{(\text{CO}_2)}$ at Etna are always remarkably more positive than MORB ones, as they reach values as high as -1‰. Such isotopic characteristics have been generally explained in terms of strong crustal contamination of a MORB-type source (Allard 1983; Allard et al. 1997; Tedesco 1997). However, according to other studies (Marty et al. 1994; D'Alessandro et al. 1997b; Nakai et al. 1997; Giammanco et al. 1998a) the observed $\delta^{13}\text{C}_{(\text{CO}_2)}$ values would be peculiar of the mantle source of gas beneath Mt. Etna, thus making this source significantly different from MORBs. In particular, Nakai et al. (1997) investigated the isotopic features of noble gases

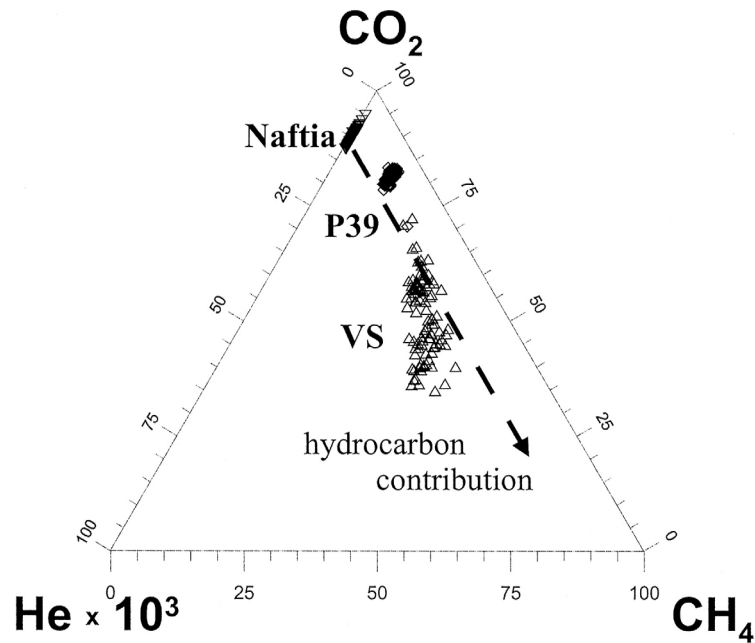


Fig. 2. He - CO₂ - CH₄ triangular plot for the CO₂-rich samples collected at Mt. Etna. This plot highlights the enrichment both in He and in CH₄ due to interaction between CO₂-rich gases and local ground waters. For samples from P39 and VS, input of CH₄ from a hydrocarbon reservoir (“hydrocarbon contribution” line in the plot) is also assumed (◆ P39; △ VS; ▽ Naftia).

derived from the mantle beneath Etna’s magmatic system, showing that the isotopic signature of He in Etna’s magma only partly overlaps the lower range inferred for MORB-type magma (8 ± 1 R/Ra) because of “recent” mixing between a depleted upper mantle (MORB-like source) and fluids enriched in radiogenic ⁴He. Furthermore, recent determinations of the ³He/⁴He ratio in magmatic gases trapped at depth into olivine crystals from Etna’s basalts (Marty et al. 1994) showed values ranging from 4.9 to 8.2 Ra (mean value of 6.7 ± 0.4 Ra).

In the case of carbon isotopes, a major contribution of carbonatic CO₂ from the widespread and thick layers of limestone in the sedimentary basement of Etna was often invoked to explain its atypical $\delta^{13}\text{C}_{(\text{CO}_2)}$ values (Allard 1983; Allard et al. 1991; Tedesco 1997). However, according to other recent studies (D’Alessandro et al. 1997b; Giammanco et al. 1998a), there is no significant contribution from CO₂ derived from heated carbonate sediments of Etna’s basement. According to Allard et al. (1997) the carbon isotopic composition of magmatic CO₂ from Etna is about -4‰. Conversely, Giammanco et al. (1998a), on the basis of the temporal correlation between volcanic activity and variations both of $\delta^{13}\text{C}_{(\text{CO}_2)}$ and CO₂ fluxes measured in sites of focused degassing, indicated $\delta^{13}\text{C}_{(\text{CO}_2)}$ values of deep magmatic gas in the

range -2 to -1 ‰. Deviations from the mantle values of $\delta^{13}\text{C}_{(\text{CO}_2)}$ in gas emissions at the surface were explained as caused by interaction between deep CO_2 and shallow fluids, such as cold and thermal ground water as well as biogenic gases (Giammanco et al. 1998a). In this case, an important role is played by the flux of CO_2 coming from depth (the higher the flux of CO_2 , the lesser the interaction between magmatic CO_2 and the surrounding environment; Giammanco et al. 1998a).

A final solution to the question of the pristine magmatic value or carbon isotopes at Etna would come from the analysis of CO_2 trapped into fluid inclusions. Unfortunately, no such data are available, mainly because of the difficulty in finding fluid inclusions into Etna's volcanics that are suitable for isotopic analyses of carbon. Furthermore, it is highly probable that any CO_2 found in fluid inclusion would be strongly fractionated isotopically because CO_2 has an early exsolution in magma caused by its low solubility in silicate melts (Stolper and Holloway, 1988). In order to find support in favour of either one of the above hypotheses on the isotopic marker of magmatic CO_2 at Etna, we used the graphic method (Fig. 3) proposed by Inguaggiato et al. (2000) applied to $\delta^{13}\text{C}_{(\text{TDIC})}$ values in groundwater samples from the Paternò area collected in recent years (Allard et al. 1997; D'Alessandro et al. 1997). The $\delta^{13}\text{C}$ values of TDIC of Etna's groundwaters measured by Allard et al. (1997) were plotted versus the corresponding values of $\text{HCO}_3^-/\text{TDIC}$ molar ratio. The graph allows to estimate the pristine isotopic composition of C of CO_2 gas that has interacted with the aquifer. The

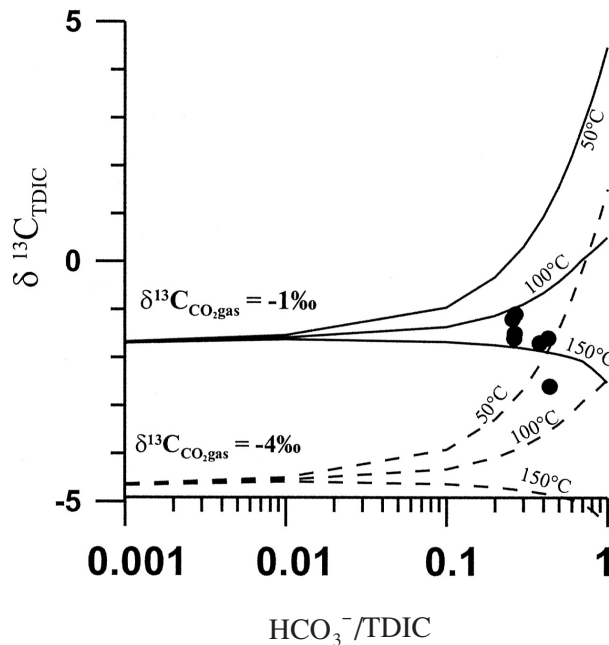


Fig. 3. Isotope composition of $\delta^{13}\text{C}_{(\text{TDIC})}$ vs. $\text{HCO}_3^-/\text{TDIC}$ ratio at values of initial $\delta^{13}\text{C}$ of CO_2 gas of -1 ‰ and -4 ‰.

range -2 to -1 ‰. Deviations from the mantle values of $\delta^{13}\text{C}_{(\text{CO}_2)}$ in gas emissions at the surface were explained as caused by interaction between deep CO_2 and shallow fluids, such as cold and thermal ground water as well as biogenic gases (Giammanco et al. 1998a). In this case, an important role is played by the flux of CO_2 coming from depth (the higher the flux of CO_2 , the lesser the interaction between magmatic CO_2 and the surrounding environment; Giammanco et al. 1998a).

A final solution to the question of the pristine magmatic value or carbon isotopes at Etna would come from the analysis of CO_2 trapped into fluid inclusions. Unfortunately, no such data are available, mainly because of the difficulty in finding fluid inclusions into Etna's volcanics that are suitable for isotopic analyses of carbon. Furthermore, it is highly probable that any CO_2 found in fluid inclusion would be strongly fractionated isotopically because CO_2 has an early exsolution in magma caused by its low solubility in silicate melts (Stolper and Holloway, 1988). In order to find support in favour of either one of the above hypotheses on the isotopic marker of magmatic CO_2 at Etna, we used the graphic method (Fig. 3) proposed by Inguaggiato et al. (2000) applied to $\delta^{13}\text{C}_{(\text{TDIC})}$ values in groundwater samples from the Paternò area collected in recent years (Allard et al. 1997; D'Alessandro et al. 1997). The $\delta^{13}\text{C}$ values of TDIC of Etna's groundwaters measured by Allard et al. (1997) were plotted versus the corresponding values of $\text{HCO}_3^-/\text{TDIC}$ molar ratio. The graph allows to estimate the pristine isotopic composition of C of CO_2 gas that has interacted with the aquifer. The

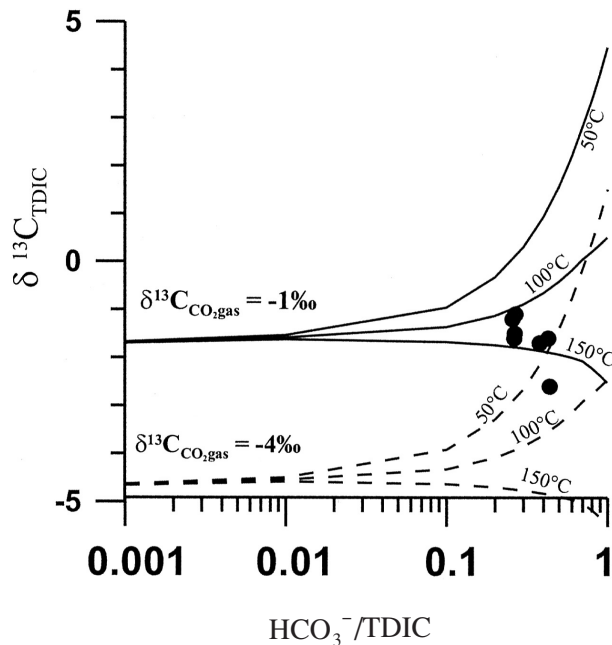


Fig. 3. Isotope composition of $\delta^{13}\text{C}_{(\text{TDIC})}$ vs. $\text{HCO}_3^-/\text{TDIC}$ ratio at values of initial $\delta^{13}\text{C}$ of CO_2 gas of -1 ‰ and -4 ‰.

curves in the plot represent the theoretical $\delta^{13}\text{C}_{(\text{TDC})}$ values calculated as a function both of temperature and of carbon molar ratio in water. Assuming initial magmatic $\delta^{13}\text{C}_{(\text{CO}_2)}$ values of -4‰ , the resulting data points fall on curves corresponding to equilibration temperatures of about 50°C . On the contrary, assuming a $\delta^{13}\text{C}_{(\text{CO}_2)}$ of -1‰ almost all of the points fall between the curves corresponding to the equilibrium temperatures of 100°C and 150°C . These temperature values match those deduced by Chiodini et al. (1996) on the basis of geothermometric estimates on gases and waters collected in the same area.

Lastly, it is generally accepted that any contribution of He and organic C from the crust to the gases emitted from fumaroles and focused degassing sites in the Etna area is negligible (Allard et al. 1997; D'Alessandro et al. 1997b; Giammanco et al. 1998a). In this work we will therefore consider magmatic values of He of about 6.7 ± 0.4 Ra, and values of $\delta^{13}\text{C}_{(\text{CO}_2)}$ in the range -2 to -1‰ , in agreement with the hypothesis formulated by Giammanco et al. (1998a).

6.2 Isotopic Composition of Gases During the Period 2000-2003

Isotope analyses on $\delta^{13}\text{C}_{(\text{CO}_2)}$ and He in the gases sampled during the period of this study showed values ranging from -22 to $+1.6\text{‰}$ and from 1.2 to 7.5 Ra, respectively (Table 1). The variability of both parameters, both among different sites and within the same site, may be a consequence of mixing between deep gas and atmosphere, as in the case of He, and/or isotopic fractionation in the case of carbon, as above described (Fig. 4). Contrary to what stated by Allard et al. (1997), we may rule out isotopic exchange between C of magmatic CO_2 and C of atmospheric CO_2 , because of the lack of correlation ($0.017 < R < 0.37$) between the measured values of N_2 and those of $\delta^{13}\text{C}_{(\text{CO}_2)}$ in the samples most contaminated with air (P78, TDF, BLV and RNE). Samples from sites BLV, TDF and RNE showed $\delta^{13}\text{C}$ values ranging from -4 to -1‰ . Because of the absence of vegetation or other organic sources of C, the most negative values at these sites can be related to CO_2 fractionated after partial dissolution of deep gas in the local cold aquifer. In these samples, the He isotope composition ranges from 1.3 to 2.4 Ra and the He/Ne ratio is around 0.4 (A. Rizzo, pers. comm.), which is an indication of marked contamination by atmospheric helium. No correction was made on the R/Ra values from these sites, however, because of the large errors involved in the calculation.

Samples from site P78 show the largest variability in $\delta^{13}\text{C}$ values (-21.7 to -2.8‰ , Table 1). According to various authors (Parello et al. 1995; Giammanco et al. 1998a), $\delta^{13}\text{C}_{(\text{CO}_2)}$ values from P78 are the result of interaction among three different C sources: i) pristine magmatic CO_2 (with carbon isotopic values between -1 and -2‰); ii) CO_2 derived from biological activity in the soil (with carbon isotopic values between -15 and -25‰); iii) CO_2 fractionated after partial dissolution of deep gas in the local aquifer at temperature lower than 120°C (because heavier carbon concentrates in the dissolved HCO_3^- ions). Giammanco et al. (1998a) observed that when soil CO_2 fluxes at P78 are low, the "organic" source becomes progressively more evident, with an isotopic shift towards more negative $\delta^{13}\text{C}$ values (up to -19‰). Conversely, when soil CO_2 fluxes are high the "magmatic" source becomes more influent. However, even in the latter case, fractionation of magmatic CO_2 due to isotopic exchange with C of HCO_3^- dissolved in ground water produces a final composition slightly more negative than that inferred for the magmatic source (Fig. 4).

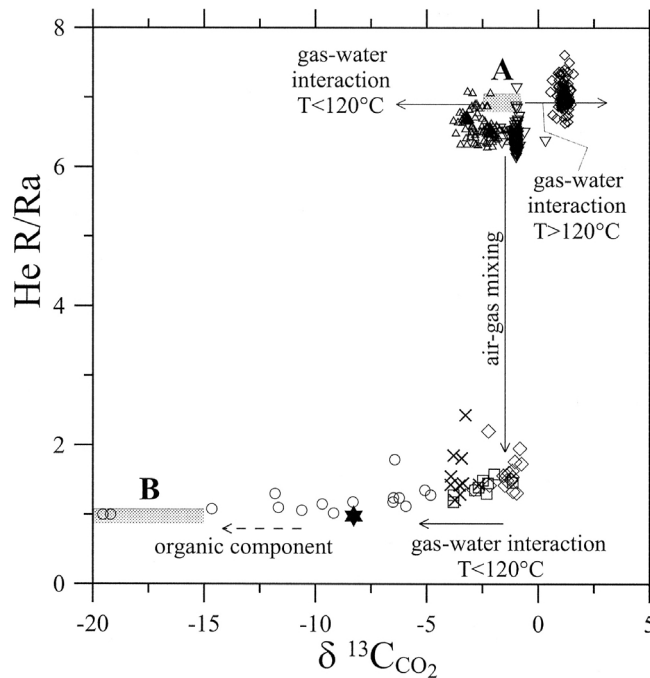


Fig. 4. R/Ra values plotted vs. $\delta^{13}\text{C}_{(\text{CO}_2)}$ values in the sampled gases. Arrows indicate isotopic fractionation and/or mixing processes. Grey box labelled **A** represents the compositional range of magmatic gas at Mt. Etna. Grey box labelled **B** represents the compositional range of the organic component. Symbol ★ indicates the isotopic composition of air (◆ P39; △ VS; ▽ Naftia; ✕ RNE; □ TDF; ◇ BLV; ○ P78).

Samples from sites P39, VS and Naftia show very similar He isotope values. R/Ra values range, respectively, from 6.7 to 7.5, from 6.5 to 7.1 and from 6.2 to 7.2 (Table 1). These values are all compatible with a magmatic origin of He (Nakai et al. 1997). Conversely, $\delta^{13}\text{C}_{(\text{CO}_2)}$ values in these samples differ markedly from one site to the other. Samples from site Naftia were characterized by very stable $\delta^{13}\text{C}$ values (around -1‰). Such isotopic composition indicates a strong contribution of deep magmatic CO_2 (De Gregorio et al. 2002). The low variability of isotopic values of C and He at this site seems to indicate very low or even no interaction with ground water, in apparent contrast with the indication from the chemical features of the emitted gases. This can be explained considering the huge flux of CO_2 (about 200 t/d) issuing from the Naftia vent; such a large amount of CO_2 prevents any significant isotopic exchange between deep carbon gas and carbon dissolved into shallow aquifers, although permitting some degree of chemical interaction. Samples from site P39 showed $\delta^{13}\text{C}$ values in the range 0.5 to 1.6‰. Such positive values are consequence of isotopic fractionation of carbon due to interaction between magmatic CO_2 and thermal groundwater at temperature $> 120^\circ\text{C}$ (Giammanco et al. 1998a), which favours ^{13}C enrichment in the residual gas phase.

Samples from site VS showed $\delta^{13}\text{C}_{(\text{CO}_2)}$ values ranging from -3.8 to -1.4‰ (Table 1). The slightly more negative values from this site relative to the others in this group could be the result of interaction between magmatic CO_2 and cold groundwater, similar to what described for site P78.

7. TEMPORAL VARIATIONS OF GEOCHEMICAL PARAMETRES

7.1 General Considerations

During the period July 2000 - July 2003 (Figs. 5 - 12) large variations were observed in the chemical and isotopic composition of sampled gases, as well as in the efflux of CO_2 through the soil, at all of the sampled sites. Anomalous changes were also recorded in the outlet temperature of the sampled fumaroles. Comparison of geochemical data with local atmospheric parametres concurrently acquired showed that only air temperature had an apparent effect on CO_2 dynamic concentration ($R^2 = 0.55$), on soil CO_2 concentration ($R^2 = 0.48$) measured at site P78, as well as on soil temperature measured at site TDF ($R^2 = 0.55$). In the case of TDF, the computation was made without taking into account the two very high values recorded in May and June 2003, because they are almost certainly due to residual cooling of the nearby magma dike of the 2002-03 eruption. No other significant correlation was found between atmospheric and geochemical parametres as noticed in other volcanic systems (Tatum Volcano Group in Northern Taiwan, Lee et al. 2005). The parameters that were found correlated with air temperature were filtered for the seasonal influence. Soil CO_2 data from P78 were filtered and normalized following a procedure similar to that used by Giammanco et al. (1995) and also by Bruno et al. (2001). Soil temperature data from TDF were filtered by simply subtracting the relevant air temperature values. All the filtered data above described will be used in the following discussion.

7.2 Variations in the CO_2 -Rich Sites (Naftia, P39, VS)

Both at P39 and at VS CO_2 is anticorrelated with He as well as with CH_4 , and this evidence was first reported by Giammanco et al. (1998a). In particular, Giammanco et al. (1998a) used the observed anticorrelation between CO_2 and CH_4 to derive the different origin of the two gases. Because the source of CH_4 is a slowly depleting, shallow hydrocarbon reservoir, it releases gas at a rate that can be considered constant, at least in the time span of some years. Therefore, as specified above, any variation in CH_4 emission at the surface is only due to changes in the flux of magmatic CO_2 that interacts with the CH_4 reservoir.

Without taking into account the few very low values due to strong air contamination of our samples (Table 1), the entity of the temporal variations of CO_2 concentration at sites Naftia, P39 and VS during the studied period (Fig. 5) was minimal in the site with the highest average CO_2 content (Naftia) and greatest in the site with lowest average CO_2 concentration (VS). However, some common patterns can be recognised at all of these sites. In general, relatively higher CO_2 values were observed in late year 2000 at Naftia and VS. Some samples

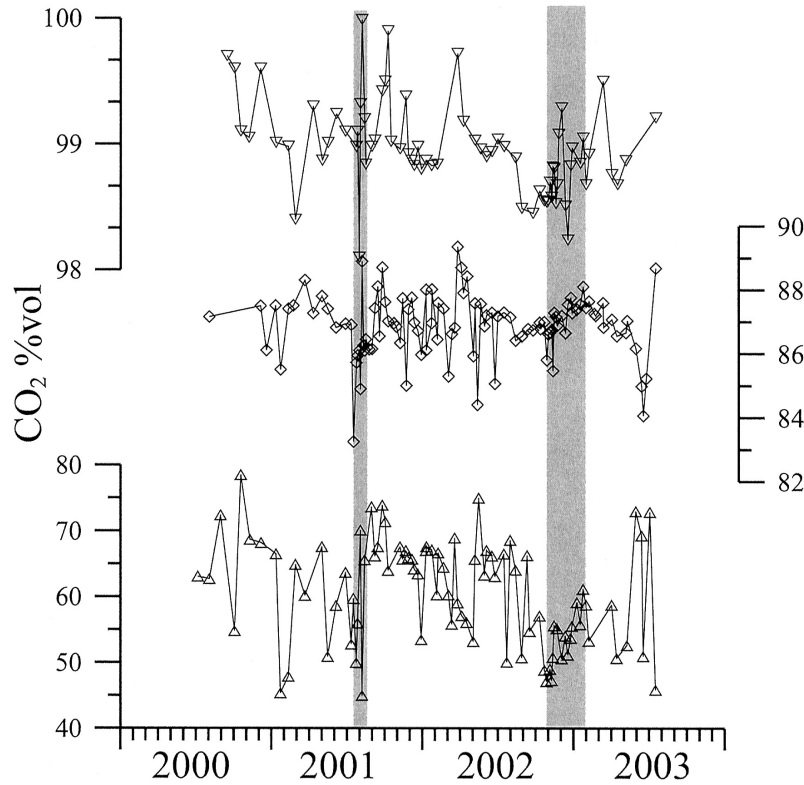


Fig. 5. Temporal variations of CO₂ concentration in the CO₂-rich sites during the studied period. Grey bars indicate the main lateral eruptions of Mt. Etna (◆ P39; △ VS; ▽ Naftia).

collected from P39 during the same period showed a strong air pollution due to some problems during gas sampling (the ground was saturated with water spilling out of a nearby channel), and have not been plotted in the graph of Fig. 5. Therefore, information on the pattern of CO₂ at this site during late 2000 is largely incomplete. Since December 2000 we moved our sampling point at P39 just a few meters away from the previous one, in dry soil. Concentrations of CO₂ higher than the respective normal values were again observed at all sites right after the end of the July-August 2001 eruption, in particular from late August to November 2001, then in March-April 2002, from December 2002 to January 2003 and lastly from May to June 2003. Increases of CO₂ content in the gases emitted from these sites suggest increase of magmatic gas pressure at great depth, probably in the deepest magma reservoir inferred from geophysical and geochemical data. Conversely, decreases in CO₂ concentration, such as those observed at all these sites before the 2001 eruption, should indicate rapid depressurisation at depth due to transfer of magma to the upper intermediate reservoir.

Carbon monoxide (Fig. 6a) was practically absent at all points until mid-June 2001, that is about one month before the 2001 eruption. During the same period H_2 was high only at P39, but decreased to air values already at the end of 2000 (Fig. 6b). Conversely, after mid-June 2001 CO was frequently observed, although with variable intensity and always with a spike-like character. Almost the same behaviour characterized the H_2 values at P39 and VS, whereas

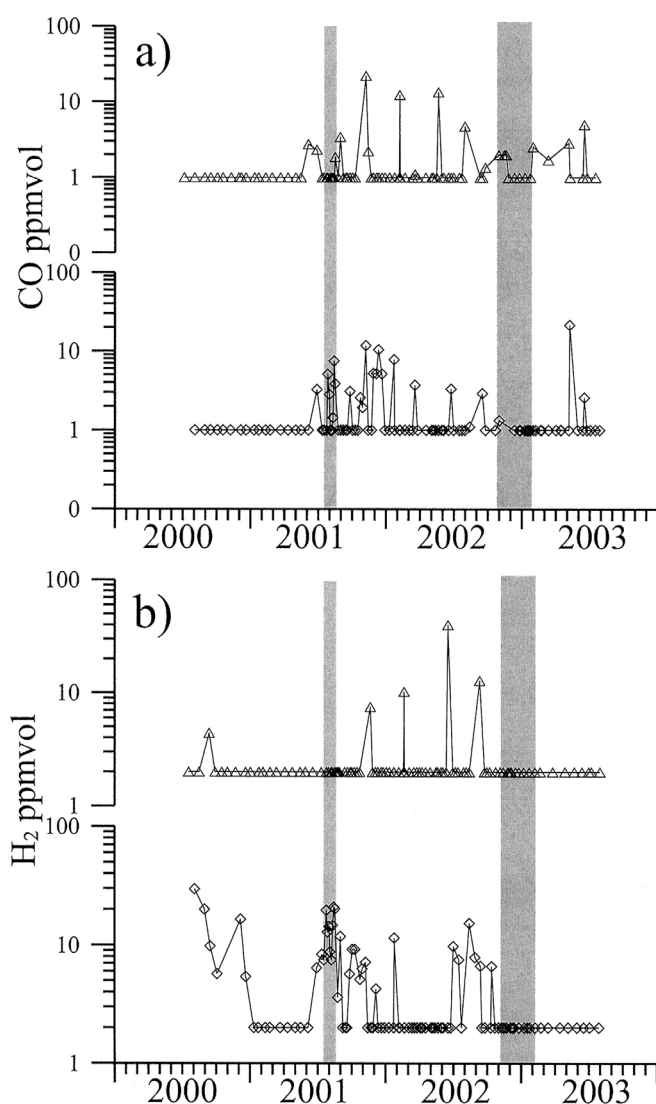


Fig. 6. Temporal variations of a) CO concentration and b) H_2 concentration in the CO_2 -rich sites during the studied period. Grey bars indicate the main lateral eruptions of Mt. Etna (\diamond P39; \triangle VS).

at Naftìa H_2 was always absent. Sites P39 and VS were also characterised by significant variations of $\delta^{13}C$ values (Fig. 7). Particularly at site VS more positive $\delta^{13}C$ values, closer to those inferred for Etna's magmatic source, were measured in the first months of 2001. At the end of the 2001 eruption $\delta^{13}C$ values became markedly negative, but soon after an increasing trend was observed, although with oscillations. This trend ended at the beginning of the 2002-03 eruption, when values stabilized close to -2.0‰ . Similar values were on average measured until the end of our observations. The variations in the $\delta^{13}C$ values observed at Naftìa were instead very small and stable around -1‰ . The He isotopic values (R/Ra) measured were generally higher at all these sites (Fig. 8) until the beginning of 2002, with highest values during the 2001 eruption. Significantly lower R/Ra values were recorded afterwards. In both periods, several sequences of negative peaks immediately followed by positive peaks were observed in all sites. According to the degassing model proposed by Nuccio and Valenza (1998) and later developed for the Etna area by Caracausi et al. (2003a, b), sequences of minima in the R/Ra values soon followed by maxima are to be interpreted as single episodes of magma ascent. The isotopic composition of the emitted helium results from the balance be-

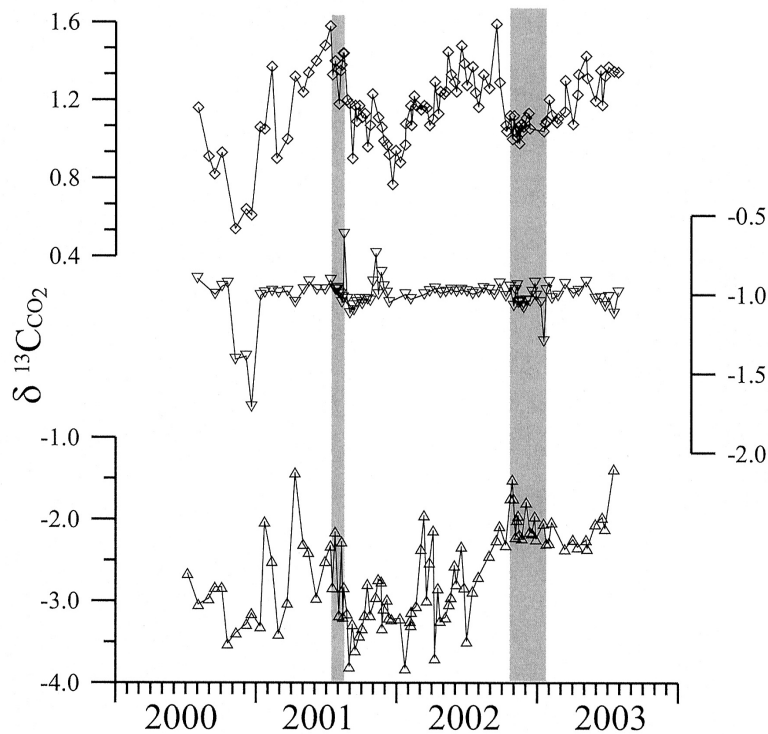


Fig. 7. Temporal variations of $\delta^{13}C_{(CO_2)}$ values in the CO_2 -rich sites during the studied period. Grey bars indicate the main lateral eruptions of Mt. Etna (\blacklozenge P39; \triangle VS; ∇ Naftìa).

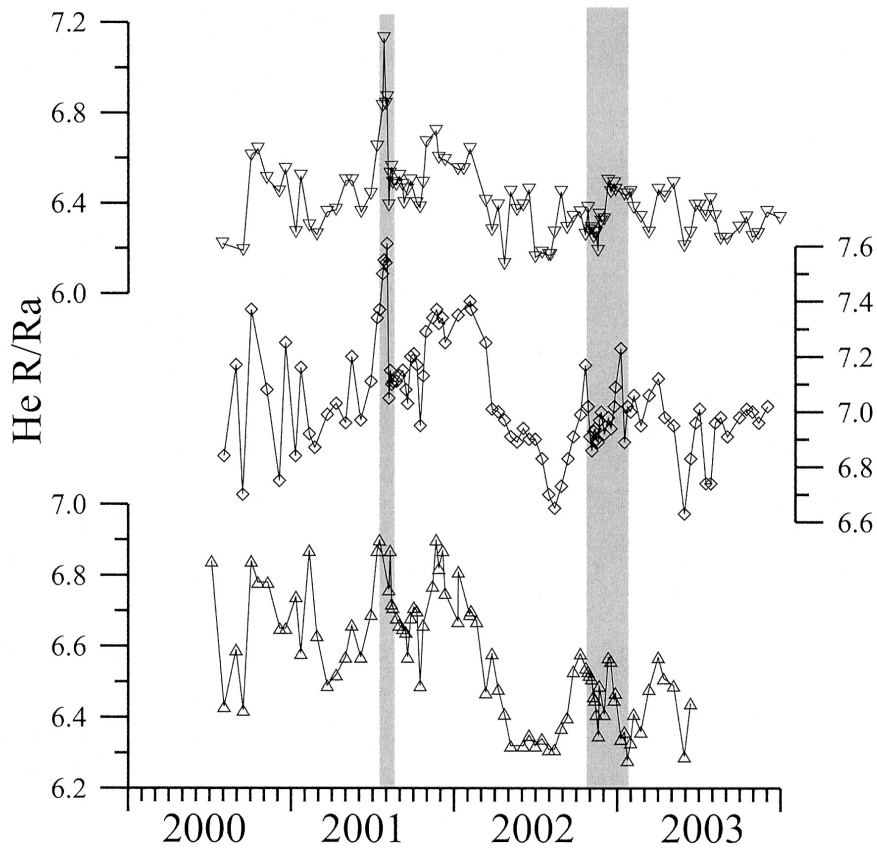


Fig. 8. Temporal variations of R/Ra values in the CO₂-rich sites during the studied period. Grey bars indicate the main lateral eruptions of Mt. Etna (◆ P39; △ VS; ▽ Naftia).

tween He released from less degassed magmas, marked by a high $^3\text{He}/^4\text{He}$ ratio, and ^3He -depleted gases coming from more degassed melt. The higher R/Ra values before 2002 indicate important accumulation of new volatile-rich magma at relatively deep levels of the Etnean volcanic system. In particular, Caracausi et al. (2003a) recognised the ascent of a batch of fresh magma at depth between May and June 2001. The significant general decrease in the R/Ra values after early 2002 would be caused by important migration of magma towards the uppermost portions of the volcano, a possible indication of the following eruptive activity of 2002 - 2003. After early 2002, other sharp variations were observed in the R/Ra values, such as in summer of 2002 and in May-June 2003, which can be interpreted as new arrivals of gas-rich melts at depth. However, these magmatic episodes did not seem to be volumetrically important, because they did not induce an appreciable increase in the average R/Ra values.

7.3 Variations in the Air-Contaminated Sites (P78, BLV, TDF, RNE)

In these sites the most evident anomalous changes were observed in the CO₂ emissions, in the CO and CH₄ concentrations and in the fumarole temperature. A good correlation can be found between soil CO₂ contents and soil CO₂ dynamic concentrations. As regards the CO₂ emissions (Fig. 9), many anomalous values were recorded throughout the study period. This indicates the occurrence of repeated episodes of intrusion and upward migration of CO₂-rich magma within the shallowest portions of Etna's feeder system. It is to be noted that anomalous

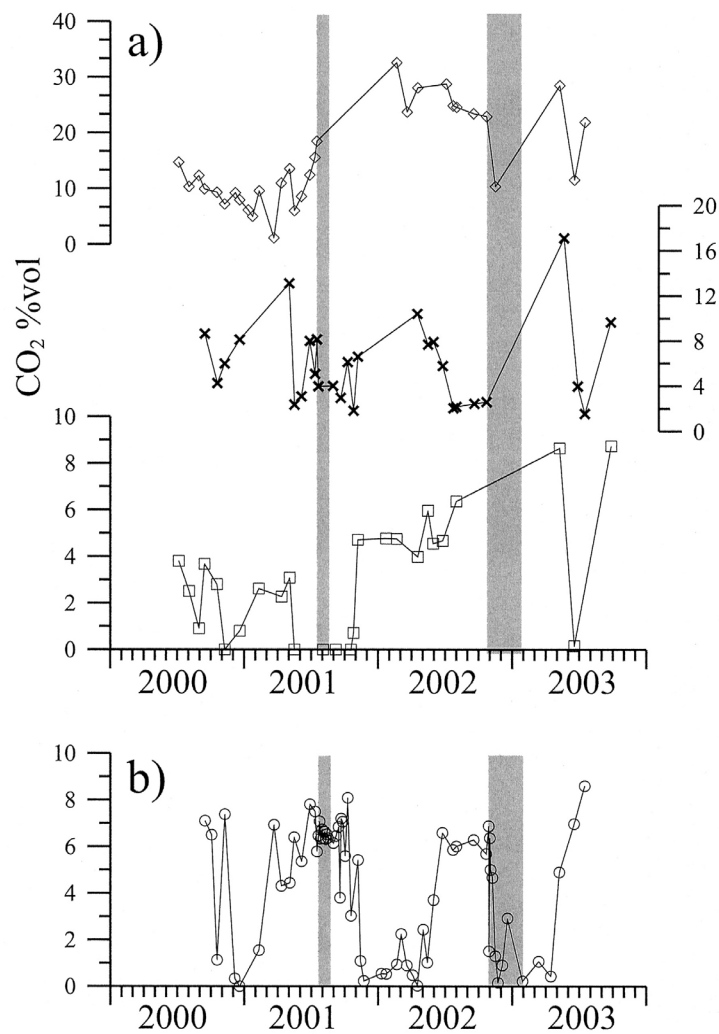


Fig. 9. Temporal variations of CO₂ concentrations at a) high-altitude sites and b) P78 during the studied period. Grey bars indicate the main lateral eruptions of Mt. Etna (X RNE; □ TDF; ◇ BLV; ○ P78).

increases in CO₂ emission at P78 occurred before those at the other sites located at higher altitude on the volcano. This is compatible with a progressive upward migration of magma towards the uppermost part of the volcanic system.

The temporal behaviour of CO at the air-contaminated sites (Fig. 10) was quite similar to that observed at the CO₂-rich sites: almost no CO emission was recorded before mid-June 2001, whereas after that moment CO was often found. Differently from the CO₂-rich sites, however, from March-April 2002 until the end of the study period CO contents were almost constantly high and showed two sudden increases followed by a slow decreasing trend. In

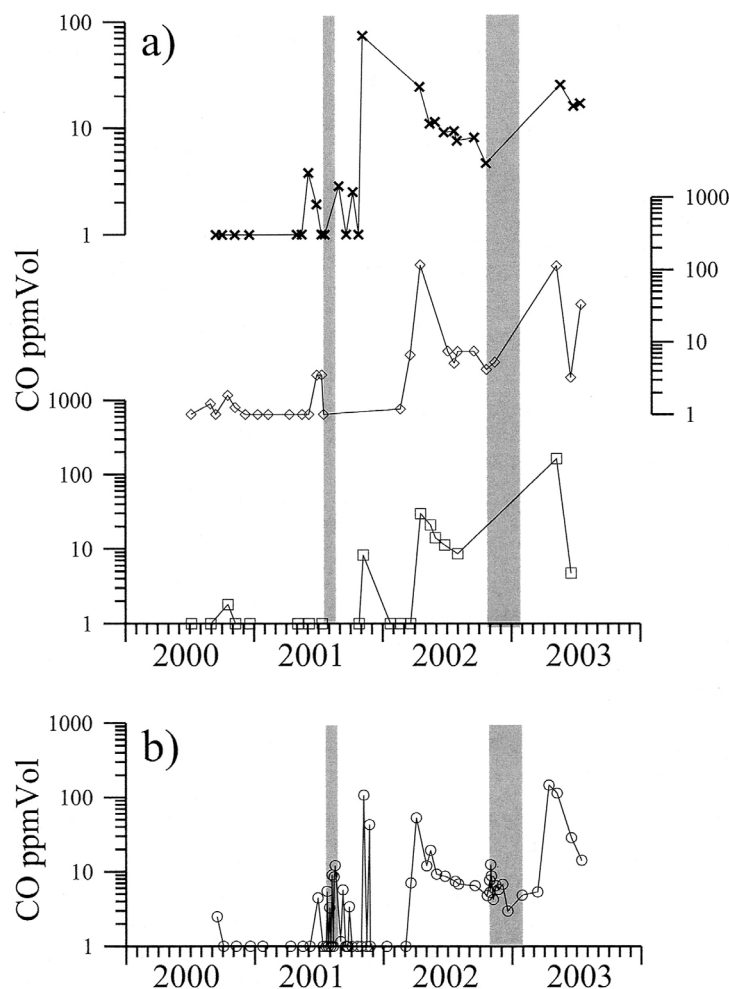


Fig. 10. Temporal variations of CO concentrations at a) high-altitude sites and b) P78 during the studied period. Grey bars indicate the main lateral eruptions of Mt. Etna (X RNE; □ TDF; ◇ BLV; ○ P78).

particular, the onset of these two anomalies (March - April 2002 and March - April 2003) coincide with anomalous high CO₂ and CH₄ emissions in the same sites. This would strengthen the hypothesis of arrival of fresh magma in the shallowest portions of Etna's feeder system, but differently from what observed before March 2002, a higher gas velocity, probably related to a higher gas pressure, has to be invoked to justify the constantly high emission of such a fast reacting and fast re-equilibrating gas species as CO (Giggenbach 1991). It must be noted that the anomalies in CO concentrations continued both during and after the occurrence of the 2002 - 03 eruption. This would suggest that magmatic pressure kept accumulating inside the volcano despite that lateral eruption.

Values of $\delta^{13}\text{C}$ at site P78, as already described, showed the strongest positive shift when soil CO₂ emissions were highest. In the other sites of this group carbon isotopes showed quite synchronous variations, although with different intensities. In these sites, $\delta^{13}\text{C}$ values shifted towards those inferred for the magmatic source of Etna not only right before the two main eruptions, but also in November 2001 and in May 2002 (Fig. 11).

The temporal changes in fumarole temperature at RNE and BLV (Fig. 12) showed similar anomalous periods as for the other parameters. It is to be noted that site BLV temperature values recorded between the two lateral eruptions were constantly higher than the background values measured before the 2001 eruption and after the 2002 - 03 eruption. In the same site it is worth mentioning the very high temperature value measured in June 2003, which well exceeded the boiling temperature of water at that altitude and would indicate a particularly strong input of high-enthalpy fluids in the shallow water table beneath the site. Temperature values at TDF, after filtering from the influence of air temperature, show a higher mean (+3.8 °C) during the period July 2000 - January 2002 compared to that of the following period (-1.9°C), without taking into account the very high values measured in may and June 2003.

8. DISCUSSIONS AND CONCLUSIONS

As a general rule, variations in the concentration and/or flux of gases issuing from the flanks of active or quiescent volcanoes can be due basically to changes in two different types of factors: environmental or volcanic. Environmental factors include atmospheric parameters such as air temperature, barometric pressure, air humidity, wind speed, rain or snow fall. These are normally characterised by periodic variations (daily, seasonal, etc.) that may be reflected in the variations of some geochemical parameters, particularly in sites with relatively low gas efflux (Hinkle 1990; Giammanco et al. 1995). Other influencing environmental parameters are those linked to the characteristics of the ground through which the gases diffuse or flow. Some of these characteristics depend on atmospheric factors: for example, soil permeability may change as a function of rain fall, which may heavily increase the amount of pore water; furthermore, rain water infiltrates and feeds underground aquifers, whose presence and volume can trigger and govern the interaction between groundwater and deep gas. Volcanic factors include increases in the efflux of magmatic fluids due to upward motion of gas-rich magma and its consequent progressive saturation in, and release of, the least soluble gas species. In particular, impulsive increases in the emission of reduced gas species (mostly H₂ and CO)

may be due to disequilibrium conditions in the gas phase dissolved in the magma imposed by a rapid migration of magma towards shallower and more oxidised portions of crust (e.g., Sato and McGee 1981; Sato 1988; Giammanco et al. 1998a).

According to recent geochemical models based on the relations between gas bubbles formation and migration within magma and velocity of magma migration within the volcanic edifice (Giammanco et al. 1995, 1998a; Nuccio and Valenza 1998; Bruno et al. 2001), increases in the emission of CO_2 from the flanks of the volcanic edifice (in fumaroles and soil emissions) would indicate higher gas release from a deep source due to increased exsolution

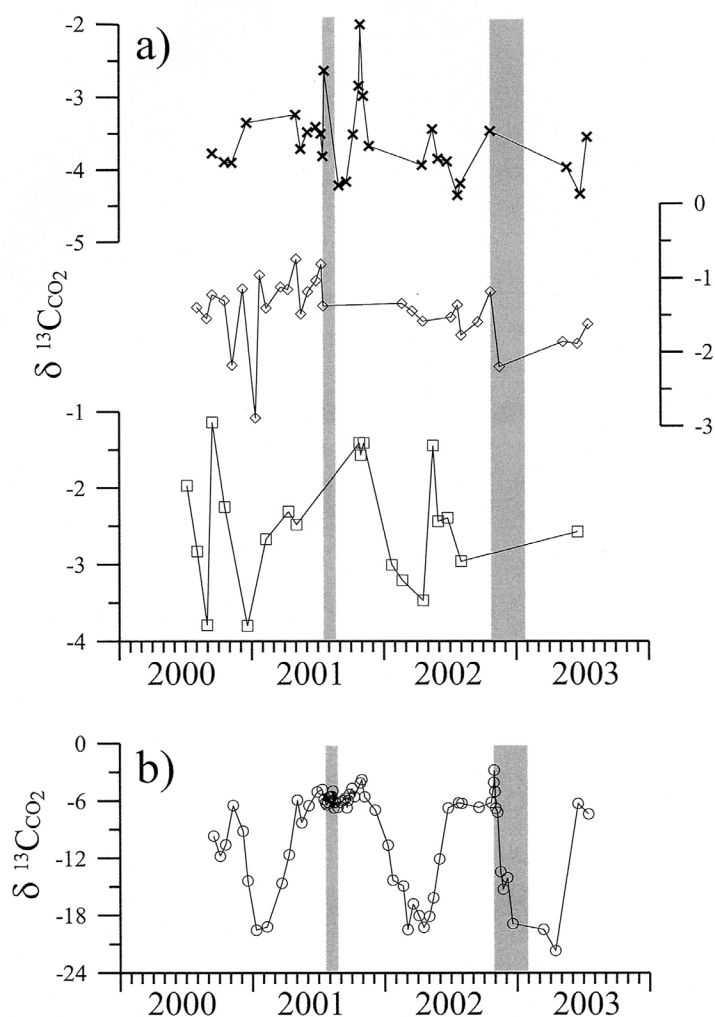


Fig. 11. Temporal variations of $\delta^{13}\text{C}_{(\text{CO}_2)}$ values in the N_2 -rich sites during the studied period. Grey bars indicate the main lateral eruptions of Mt. Etna (✕ RNE; □ TDF; ◇ BLV; ○ P78).

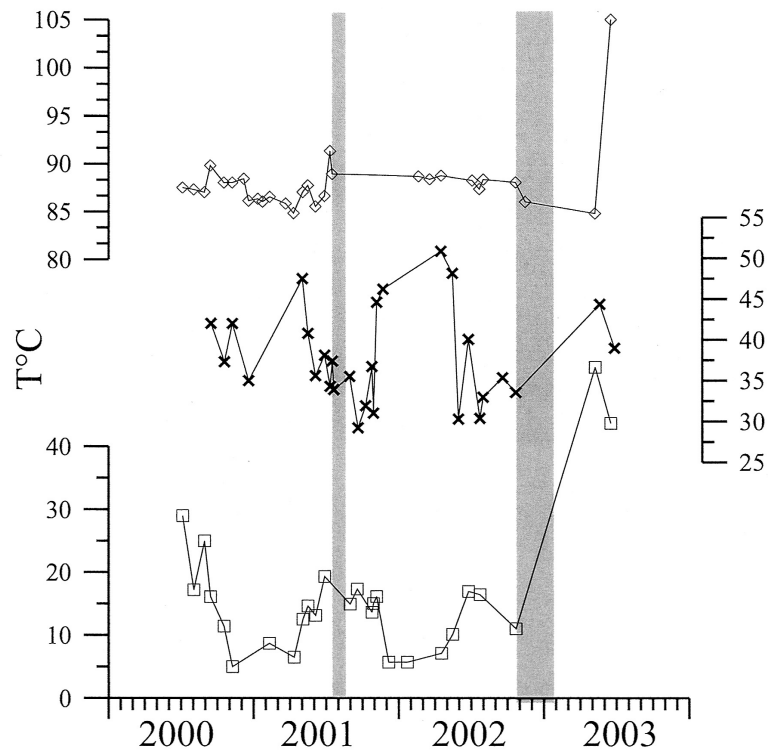


Fig. 12. Temporal variations of fumarole temperature values at BLV, TDF and RNE during the studied period (X RNE; □ TDF; ◇ BLV; ○ P78). Values from TDF were filtered from the seasonal variations (see text). Grey bars indicate the main lateral eruptions of Mt. Etna.

of gas from an ascending, gas-rich magma. Furthermore, sudden and/or marked decreases can be ascribed to rapid magma migration within the volcanic edifice, either upwards or laterally.

During the period July 2000 - July 2003, five periods of marked anomalies were recognized: August - December 2000, April - September 2001, October - December 2001, April - November 2002 and May - June 2003. Because of the general lack of environmental influences on the entity and variation of parietal degassing at Mt. Etna, the observed anomalous signals are coherent in indicating as increased magmatic degassing from an up-rising body of fresh magma. Occurrence of gas anomalies in the majority, if not in all, of the sites, some of which located at great linear distance (up to 50 km) one from the other, suggests increase of magmatic gas pressure in a deep magma reservoir beneath Mt. Etna. This reservoir probably corresponds to the deepest one (> 10 km depth) inferred from geophysical and geochemical data. The large width of this magma reservoir, indicated by Caracausi et al. (2003a) to be about 60 km, was hypothesised to explain the almost synchronous variations in the isotope composition of He observed in sites located both at the foot of Etna (P39 and VS) and almost 40 km away from its

boundary (Naftia). According to Caracausi et al. (2003a), the site Naftia with its huge emission of CO₂ is directly linked to an active magma intrusion in the uppermost 30 km of crust. More recently, Caracausi et al. (2003b), based on the computed pressures for the gases feeding the Naftia emissions, invoked the presence of magma into dikes that probably extend up to 3 - 4 km beneath the surface and are frequently replenished with fresh magma. Support to this assumption came from the reported high heat fluxes (up to 100 mW m⁻², according to Cataldi et al. 1995; Barbier et al. 1998) close to this site, along a fault system directed NE-SW.

In our opinion, an alternative model is that the site Naftia is the surface expression of a "gas dike" formed into the lithospheric NE-SW-trending faults. According to Carrigan (2000), a gas dike can form when hydraulic fracturing induced by hot magmatic gas under pressure causes crustal breaking and the fracture is kept open. In the case of magma intrusion, the following applies:

$$P_{tip_{mag}} = P_{mag} - \rho_{mag} g l \ll P_{mag} \quad , \quad (1)$$

in which $P_{tip_{mag}}$ is the pressure in the fill magma fracture tip, ρ_{mag} is the magma density, g is the gravity acceleration and l is the fracture length. According to Eq. (1), due to the high density of magma the pressure at the fracture tip is much lower than at depth where the intrusion started. Conversely, in the case of a gas dike, the following applies:

$$P_{tip_{gas}} = P_{mag} - \rho_{gas} g l \approx P_{mag} \quad , \quad (2)$$

in which $P_{tip_{gas}}$ is the pressure in the fill gas fracture tip, ρ_{gas} is the gas density. Eq. (2) shows that due to the very low density of gas, the pressure at the fracture tip is almost the same as that at depth. In this case it is highly probable that pressurized gas impedes the uprise of magma within the fracture. This model justifies the remarkable gas fluxes observed at the surface at site Naftia, and also means that the gas dike feeding Naftia is continuously and adequately replenished with new gas from the deep magma reservoir. This model also explains the anomalous heat fluxes measured around the Naftia area, the stable $\delta^{13}C$ values around the magmatic ones and the almost synchronous temporal variation observed in the He isotopes from Naftia and from the sites of the lower SW flank of Etna, because heat can be efficiently carried by high-flux, water-rich gases. Furthermore, pressure waves produced by increased degassing of deep magma can propagate much faster through a gas than through a silicate melt, and hence they can be observed with a short time lag even at great distances from the magma source. Lastly, further support to this model comes from the geophysical data from the Naftia area, because no seismic activity has occurred there in recent years and hence there is no physical evidence of active magma intrusions at shallow depth (S. Alparone pers. comm.).

Upon rising towards the surface after their release from melt, the magmatic gases undergo several geochemical processes, which determine the final chemical and isotopic composition of all gas emissions collected at Mt. Etna (Fig. 13):

i) interaction between magmatic gases and shallow ground water, which causes enrichment of

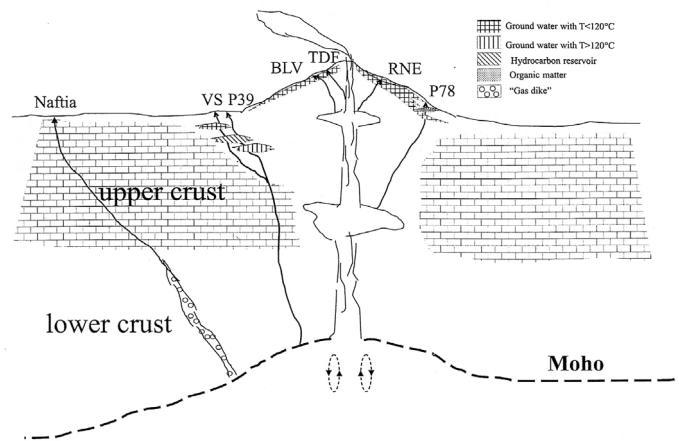


Fig. 13. Schematic cross section of Mt. Etna. Sampled gas emissions are also indicated. In this picture are schematically shown the hypothesised interactions that magmatic gases undergo during their upflow.

- the residual gas fraction in the least soluble species, such as He and CH_4 , and isotopic shift of C of residual CO_2 , whose sign is a function both of water temperature and CO_2 flux;
- ii) interaction between magmatic gases and light hydrocarbons, which adds CH_4 to the uprising gas, as in the case of P39 and VS;
 - iii) interaction between magmatic gases and organic matter, which causes a strong negative isotopic shift of $\delta^{13}\text{C}_{(\text{CO}_2)}$, as in the case of P78.

All the sampled sites show evident temporal anomalies both in the chemical and in the isotopic parameters during the studied period although with different amplitude. The gases issuing from the most peripheral sites, in particular CO_2 , were largely buffered by local ground water, and the entity of the anomalous variations of some chemical parameters were damped. This process did not affect neither C nor He isotopes, as above mentioned.

All in all, the variations observed during the period under consideration indicate that the eruptive activity that occurred meanwhile was produced by magma that moved upward in many, relatively small, batches.

In conclusion, we might expect that if the volcanic system will continue to behave in the same way it did during the period of our observation, then in case of new input of magma towards the surface we should observe:

- i) anomalous changes in almost all of the chemical parameters under consideration, as well as in the outlet temperature of fumaroles;
- ii) shift of $\delta^{13}\text{C}_{(\text{CO}_2)}$ values because of increased input of magmatic CO_2 with relatively more positive isotopic values (-2 to -1 ‰);
- iii) if the amount of rising magma is relatively small, the anomalies would be larger in the sites located closer to the central axis of the volcano, which drains gases from the uppermost portions of Etna's feeding system.

According to the above statements, data collected after the end of the 2002 - 03 eruption suggested new arrival of magma at depth. This indication is in agreement with recent interpretations of geophysical data collected before and during the 2002 - 03 eruption (Patané et al. 2003). Therefore, Mt. Etna still keeps a high eruptive potential.

Acknowledgements The authors wish to thank the Ente Regionale Parco dell'Etna-Regional Park of Etna, for giving the permission to work inside protected areas. Thanks are also due to Giuseppe Riccobono, Alfio Amantia and Salvatore Carbonaro for their help during the field work, and to Walter. D'Alessandro and two anonymous reviewers for their thoughtful comments and suggestions on the manuscript.

REFERENCES

- Allard, P., 1983: The origin of water, carbon, sulfur, nitrogen, and rare gases in volcanic exhalations: evidence from isotope geochemistry. In: Tazieff, H., and J. C. Sabroux (Eds.), *Forecasting volcanic events*. Elsevier, Amsterdam, 337-386.
- Allard, P., 1986: *Geochimie isotopique et origine de l'eau, du carbone et du soufre dans les gas volcaniques: zone de rift, marges continentale set arcs insulaires*. PhD Thesiys. Université de Paris VII.
- Allard, P., 1997: Endogenous magma degassing and storage at Mount Etna. *Geophys. Res. Lett.*, **24**, 2219-2222.
- Allard, P., J. Carbonelle, D. Dajlevic, J. Le Bronec, P. Morel, M. C. Robe, J. M. Maurenas, R. Faivre-Pierret, D. Martin, J. C. Sabroux, and P. Zettwoog, 1991: Eruptive and diffuse emissions of CO₂ from Mount Etna. *Nature*, **35**, 387-391.
- Allard, P., P. Jean-Baptiste, W. D'Alessandro, F. Parello, B. Parisi, and C. Flehoc, 1997: Mantle derived helium and carbon in grounwaters and gases of Mount Etna, Italy. *Earth Planet. Sci. Lett.*, **148**, 501-516.
- Anzà, S., B. Badalamenti, S. Giammanco, S. Gurrieri, P. M. Nuccio, and M. Valenza, 1993: Preliminary study on emanation of CO₂ from soils in some areas of Mount Etna (Sicily). *Acta Vulcanol.*, **3**, 189-193.
- Aubert, M., and J. C. Baubron, 1988: Identification of a hidden thermal fissure in a volcanic terrain using a combination of hydrothermal convection indicators and soil-atmosphere analysis. *J. Volcanol. Geotherm. Res.*, **35**, 217-225.
- Barbier, E., F. Musmeci, and P. Sarocco, 1998: Banca Nazionale Dati Geotermici. Istituto Internazionale Ricerche Geotermiche, CNR Internal Report.
- Baubron, J. C., 1996: *Prospection, caractérisation et variabilité temporelle d'émanations gazeuses diffuses à l'Etna (Sicile, Italie)*. Années 1993 et 1994. Contract EV5V-CT92-0177, Rapport BRGM R 38820 dr/hgt 96. 74 p.
- Behncke, B., and M. Neri, 2003: The July - August 2001 eruption of Mt Etna (Sicily). *Bull. Volcanol.*, **65**, 461-476.
- Bonaccorso, A., R. Velardita, and L. Villari, 1994: Ground deformation modelling of geodynamic activity associated with the 1991-1993 Etna eruption. *Acta Vulcanol.*, **4**, 87-96.

- Bonaccorso, A., 1996: Dynamic inversion of ground deformation data for modelling volcanic sources (Etna 1991-1993). *Geophys. Res. Lett.*, **23**, 451-454.
- Bousquet, J. C., G. Lanzafame, and C. Paquin, 1988: Tectonic stresses and volcanism: in-situ stress measurements and neotectonic investigations in the Etna area (Italy). *Tectonophys.*, **149**, 219-231.
- Bruno, N., T. Caltabiano, and R. Romano, 1999: SO₂ emissions at Mt. Etna with particular reference to the period 1993 - 1995. *Bull. Volcanol.*, **60**, 405-411.
- Bruno, N., T. Caltabiano, S. Giammanco, and R. Romano, 2001: Degassing of SO₂ and CO₂ at Mount Etna as an indicator of pre-eruptive ascent and shallow emplacement of magma. *J. Volcanol. Geotherm. Res.*, **110**, 137-153.
- Capasso, G., and S. Inguaggiato, 1998: A simple method for the determination of dissolved gases in natural waters. An application to thermal waters from Vulcano Island. *Appl. Geochem.*, **13**, 631-642.
- Caracausi, A., R. Favara, S. Giammanco, F. Italiano, P. M. Nuccio, A. Paonita, G. Pecoraino, and A. Rizzo, 2003a: Mount Etna: Geochemical signals of magma ascent and unusually extensive plumbing system. *Geophys. Res. Lett.*, **30**, 2, 1057, doi:1029/2002GL015463.
- Caracausi, A., F. Italiano, P. M. Nuccio, A. Paonita, and A. Rizzo, 2003b: Evidence of deep magma degassing and ascent by geochemistry of peripheral gas emissions at Mount Etna (Italy): Assessment of the magmatic reservoir pressure. *J. Geophys. Res.*, **108**, B10, 2463, doi: 10.1029/2002JB002095.
- Cardaci, C., M. Coviello, G. Lombardo, G. Patanè, and R. Scarpa, 1993: Seismic tomography of Etna volcano. *J. Volcanol. Geotherm. Res.*, **56**, 357-368.
- Carrigan, C., 2000: Plumbing systems. In: Sigurdsson, H., B. F. Houghton, S. R. McNutt, H. Rymer, and J. Stix (Eds.), *Encyclopedia of Volcanoes*. Academic Press, New York, 219-235.
- Cataldi, R., F. Mongelli, P. Squarci, L. Taffi, G. Zito, and C. Calore, 1995: Geothermal ranking of Italian territory. *Geothermics*, **24**, 115-129.
- Chiodini, G., W. D'Alessandro, and F. Parello, 1996: Geochemistry of gases and waters discharged by the mud volcanoes at Paternò, Mt. Etna (Italy). *Bull. Volcanol.*, **58**, 51-58.
- Condomines, M., J. C. Tanguy, and V. Michaud, 1995: Magma dynamics at Mt. Etna: constraints from U-Th-Ra-Pb radioactive disequilibria and Sr isotopes in historical lavas. *Earth Planet. Sci. Lett.*, **132**, 25-41.
- D'Alessandro, W., R. De Domenico, F. Parello, and M. Valenza, 1992: Soil degassing in tectonically active areas of Mt. Etna. *Acta Vulcanol.*, **2**, 175-183.
- D'Alessandro, W., S. De Gregorio, G. Dongarrà, S. Gurrieri, F. Parello, and B. Parisi, 1997a: Chemical and isotopic characterization of the gases of Mount Etna (Italy). *J. Volcanol. Geotherm. Res.*, **78**, 65-76.
- D'Alessandro, W., S. Giammanco, F. Parello, and M. Valenza, 1997b: CO₂ output and $\delta^{13}\text{C}_{(\text{CO}_2)}$ from Mount Etna as indicators of degassing of shallow asthenosphere. *Bull. Volcanol.*, **58**, 455-458.
- De Gregorio, S., I. S. Diliberto, S. Giammanco, S. Gurrieri, and M. Valenza, 2002: Tectonic control over large-scale diffuse degassing in eastern Sicily (Italy). *Geofluids*, **2**, 273-284.

- Deines, P., 1970: The carbon and oxygen isotopic composition of carbonates from the Oka Carbonatite complex, Quebec, Canada. *Geochim. Cosmochim. Acta*, **34**, 1199-1225.
- Giammanco, S., S. Gurrieri, and M. Valenza, 1995: Soil CO₂ degassing on Mt. Etna (Sicily) during the period 1989-1993: discrimination between climatic and volcanic influences. *Bull. Volcanol.*, **57**, 52-60.
- Giammanco, S., S. Gurrieri, and M. Valenza, 1997: Soil CO₂ degassing along tectonic structures of Mount Etna (Sicily): the Pernicana fault. *Appl. Geochem.*, **12**, 429-436.
- Giammanco, S., S. Inguaggiato, and M. Valenza, 1998a: Soil and fumarole gases of Mount Etna: geochemistry and relations with volcanic activity. *J. Volcanol. Geotherm. Res.*, **81**, 297-310.
- Giammanco, S., S. Gurrieri, and M. Valenza, 1998b: Anomalous soil CO₂ degassing in relation to faults and eruptive fissures on Mount Etna (Sicily, Italy). *Bull. Volcanol.*, **60**, 252-259.
- Giammanco, S., S. Gurrieri, and M. Valenza, 1999: Geochemical investigations applied to active fault detection in a volcanic area: The North-East Rift on Mt. Etna (Sicily, Italy). *Geophys. Res. Lett.*, **26**, 2005-2008.
- Giggenbach, W.F., 1991: Chemical techniques in geothermal exploration. In: D'Amore, F. (Ed.), *Application of Geochemistry in Geothermal Reservoir Development*. UNITAR, 119-144.
- Gurrieri, S., and M. Valenza, 1988: Gas transport in natural porous mediums: a method for measuring CO₂ flows from the ground in volcanic and geothermal areas. *Rend. Soc. It. Min. Petrog.*, **43**, 1151-1158.
- Gurrieri, S., S. De Gregorio, I. S. Diliberto, S. Giammanco, and M. Valenza, 1998: Soil gas emissions and tectonics in volcanic areas of Italy and Hawaii. In: Arehart, G. B., and J. R. Hulston (Eds.), *Water-Rock Interaction*. Balkema, Rotterdam, 773-776.
- Grassa, F., G. Capasso, E. Faber, S. Inguaggiato, and M. Valenza, 2004: Molecular and isotopic composition of free hydrocarbon gases from Sicily, Italy. *Geophys. Res. Lett.*, **31**, L06607, doi:10.1029/2003GL019362.
- Gvirtzman, Z., and A. Nur, 1999: The formation of Mount Etna as the consequence of slab rollback. *Nature*, **401**, 782-785.
- Hirn, A., R. Nicolich, J. Gallart, M. Laigle, and L. Cernobori, 1997: Roots of Etna volcano in faults of great earthquakes. *Earth Planet. Sci. Lett.*, **148**, 171-191.
- Hinkle, M., 1990: Factors affecting concentrations of helium and carbon dioxide in soil gases. In: Durrance, E. M., E. M. Galimov, M. E. Hinkle, G. M. Reimer, R. Sugisaki and S. S. Augustithis (Eds.), *Geochemistry of gaseous elements and compounds*. Theophrastus Pub., Athens, 421-448.
- Inguaggiato, S., G. Pecoraino, and F. D'Amore, 2000: Chemical and isotopic characterisation of fluid manifestations of Ischia island (Italy). *J. Volcanol. Geotherm. Res.*, **99**, 151-178.
- INGV-CT (Research staff of the Istituto Nazionale di Geofisica e Vulcanologia - Sezione di Catania, Italy), 2001: Multidisciplinary approach yields insight into Mt. Etna eruption. *EOS Trans. AGU*, **82**, 653-656.
- Lee, H. F., T. F. Yang, T. F. Lan, S. R. Song, and S. Tsao, 2005: Fumarolic gas compositions of the Tatun Volcano Group, northern Taiwan. *Terr. Atmos. Ocean. Sci.*, **16**, 843-864.

- Marty B., T. Trull, P. Lussiez, I. Basile, and J. C. Tanguy, 1994: He, Ar, O, Sr and Nd isotope constraints on the origin and evolution of Mount Etna magmatism. *Earth Planet. Sci. Lett.*, **126**, 23-39.
- Murray, J. B. 1990: High-level magma transport at Mount Etna volcano, as deduced from ground deformation measurements. In: Ryan, M. P. (Ed.), *Magma transport and storage*. John Wiley and Sons, New York, 357-383.
- Murru M., C. Montuori, M. Wyss, and E. Privitera, 1999: The location of magma chambers at Mt. Etna, Italy, mapped by b-values. *Geophys. Res. Lett.*, **26**, 2553-2556.
- Nakai S., H. Wakita, P. M. Nuccio, and F. Italiano, 1997: MORB-type neon in an enriched mantle beneath Etna, Sicily. *Earth Planet. Sci. Lett.*, **153**, 57-66.
- Nuccio, P. M., and M. Valenza, 1998: Magma degassing and geochemical detection of its ascent. In: Arehart, G. B., and J. R. Hulston (Eds.), *Water-Rock Interaction*. Balkema, Rotterdam, 475-478.
- Parello, F., W. D'Alessandro, P. Bonfanti, and G. Dongarrà, 1995: Subsurface gases in selected sites of the Mt. Etna area (Sicily). *Acta Vulcanol.*, **7**, 35-42.
- Patanè, D., P. De Gori, C. Chiarabba, and A. Bonaccorso, 2003: Magma Ascent and the Pressurization of Mount Etna's Volcanic System. *Science*, **299**, 2061-2063.
- Rasà, R., F. Ferrucci, S. Gresta, and D. Patanè, 1995: Etna: sistema di alimentazione profondo, assetto geostatico locale e bimodalità? di funzionamento del vulcano. In: Ferrucci, F., and F. Innocenti (Eds.), *Progetto-Etna 1993 - 1995*. Giardini, Pisa. 145-150.
- Sato, M., 1988: Continuous monitoring of hydrogen in volcanic areas: petrological rationale and early experiments. *Rend. Soc. Ital. Mineral. Petrol.*, **43**, 1265-1281.
- Sato, M., and K. A. McGee, 1981: Continuous monitoring of hydrogen on the south flank of Mount St. Helens. In: Lipman, P. W., and D. R. Mullineaux (Eds.), *The 1980 eruptions of Mount St. Helens volcano*. USGS Professional Paper 1250. 209-219.
- Sharp, A. D. L., P. M. Davis, and F. Gray, 1980: A low velocity zone beneath Mount Etna and magma storage. *Nature*, **287**, 587-591.
- Stolper, E., and J. R. Holloway, 1988: Experimental determination of the solubility of carbon dioxide in molten basalt at low pressure. *Earth Planet. Sci. Lett.*, **87**, 397-408.
- Tanguy, J. C., M. Condomines, and G. Kieffer, 1997: Evolution of the Mount Etna magma: Constraints on the present feeding system and eruptive mechanism. *J. Volcanol. Geotherm. Res.*, **75**, 221-250.
- Taylor, H. P., J. Frechen, and E. T. Degens, 1967: Oxygen and carbon isotope studies of carbonatites from the Laacher See district, West Germany and the Alnö district, Sweden. *Geochim. Cosmochim. Acta*, **31**, 407-430.
- Tedesco, D., 1997: Systematic variations in $^3\text{He}/^4\text{He}$ ratio and carbon of fumarolic fluids from active volcanic areas in Italy: Evidence for radiogenic ^4He and crustal carbon addition by the subducting African plate? *Earth Planet. Sci. Lett.*, **151**, 255-269.